Temporal regulation of green and red cone specification in human retinas and retinal organoids

Sarah E. Hadyniak[1], Kiara C. Eldred[1,°], Boris Brenerman[1], Katarzyna A. Hussey[1], Rajiv C. McCoy[1], Michael E. G. Sauria[1], James A. Kuchenbecker[2], Maureen Neitz[2], Jay Neitz[2], James Taylor[1,†], and Robert J. Johnston, Jr.[1,*]

[1] Department of Biology, Johns Hopkins University, 3400 N. Charles Street, Baltimore, MD 21218, United States

[2] Department of Ophthalmology, University of Washington, Seattle, WA, 98105, United States

° Current address: Department of Biological Structure, University of Washington, Seattle, WA, 98105, United States

† Deceased

*Corresponding author. Email: robertjohnston@jhu.edu

One sentence summary: Temporal specification of human cones

Key words: human retina, retinal organoid, photoreceptor, red cones, green cones, temporal, stochastic, opsin, retinoic acid, NR2F2

Abstract

Trichromacy is unique to primates among mammals, enabled by specification of blue (short/S), green (medium/M), and red (long/L) cones. During retinal development in humans and Old World monkeys, cones make a poorly understood choice between M and L cone subtype fates. Two nonexclusive models have been proposed: a stochastic model, in which a regulatory DNA element randomly loops to either the *M- or L-opsin* promoter to drive expression, and a temporal model, in which cone subtypes are generated in a developmental progression. Here we present data that support a temporal mechanism for M and L cone specification. *M-opsin* is expressed prior to *L-opsin* during fetal retinal development. Natural variation in the ratios of M and L cone subtypes is associated with a polymorphism in the *NR2F2* gene, a mediator of retinoic acid (RA) signaling. RA-synthesizing enzymes are highly expressed in early development and then decrease, suggesting high RA signaling early. Human retinal organoids grown in standard culture conditions were enriched for L cones, whereas early addition of RA yielded M cone-rich organoids. Our data suggest that M cones are generated before L cones and that RA signaling induces M cones and suppresses L cones early during development. These studies advance human retinal organoids as a model to study developmental processes unique to humans and primates.

Introduction

Trichromacy in humans is enabled by three subtypes of cone photoreceptors that express opsin photopigments sensitive to short (S), medium (M), or long (L) wavelengths of light[1]. Among mammals, only humans, Old World primates, and some New World monkeys have retinas with both M and L cones[2-8]. The only known difference between M and L cones is the expression of their respective opsin photopigment[9-11]. The *OPN1LW* (*L-opsin*) and *OPN1MW* (*M-opsin*) genes lie in an array on the X chromosome under the control of a shared regulatory DNA element called a locus control region (LCR)[12-14]. Though the number and ordering of *OPN1LW* and *OPN1MW* genes can vary, the LCR regulatory element is most commonly found upstream of *OPN1LW* followed by two copies of *OPN1MW* (**Fig. 1A**)[15]. Expression analyses suggested that, no matter the arrangement, only the first two opsin genes in the array are expressed in the human eye[9,12,16-19]. M and L cones have been technically challenging to distinguish due to the high sequence and structural similarity between the M- and L-opsins, and thus, the mechanisms underlying this fate decision have remained largely mysterious. Here, we examined the timing of *M-* and *L-opsin* mRNA expression during development, associated differences in M and L cone ratios with naturally occurring genomic polymorphisms in human populations, and tested mechanisms underlying specification of M and L cones in human retinal organoids to understand the developing human retina.

Two nonexclusive mechanisms have been proposed to control M and L cone generation: a stochastic model and a temporal model. In the stochastic model, the LCR randomly loops to either the *M-opsin* promoter or the *L-opsin* promoter, stably driving exclusive expression of that opsin[1,13,20]. The stochastic model is based on transgene

67 reporter experiments in mice, which showed that the probability of expression from the
68 *M-* or *L-opsin* promoters was dependent on the order and distance between the LCR and
69 opsin promoters[13]. In the temporal model, M cones are generated before L cones.
70 Functional microspectrophotometry, multifocal-ERG imaging, and expression studies
71 suggested that, compared to the early-developing central retina, the late-developing
72 peripheral retina has an increased proportion of L cones[11,21-33]. In this study, we examined
73 human retinas and retinal organoids during development to assess these mechanisms.

74 Organoids provide a powerful system to investigate the molecular mechanisms
75 controlling fate specification during human development[34,35]. We previously showed that
76 human retinal organoids generate S cones before M and L cones with similar gene
77 expression patterns and cell morphologies. We experimentally manipulated organoids to
78 identify a critical role for thyroid hormone signaling in this step of cone subtype
79 specification[36]. We thus sought to probe the organoid system to understand the primate-
80 specific fate decision between M and L cones.

81 We found that *M-opsin* is expressed earlier than *L-opsin* in human retinas. We
82 studied natural variation in M and L cone ratios in the human population and identified an
83 association with a variant in *NR2F2*, a mediator of retinoic acid (RA) signaling. We
84 analyzed a fetal RNA-seq dataset to assess expression of RA regulatory genes and found
85 high expression of RA-synthesizing enzymes early followed by a significant decrease,
86 suggesting high RA signaling early and low RA signaling late during development. To
87 distinguish between the highly similar *M-* and *L-opsin* mRNA transcripts, we developed
88 an *in situ* hybridization approach and examined expression in human retinal organoids.
89 Organoids grown in standard culture conditions were enriched for L cones, whereas

organoids supplemented with RA early in development displayed a high proportion of M cones. Our data suggest that M and L cones are specified in a temporal progression and that early RA signaling induces M cones and suppresses L cones in the developing human retina.

Results

M-opsin is expressed before *L-opsin* during human fetal retinal development

To determine the developmental dynamics of cone subtype generation, we examined the timing of *M-* and *L-opsin* expression. In a stochastic model, we predicted that *M- and L-opsin* should be expressed simultaneously throughout development. In a temporal model, one opsin should be expressed before the other opsin.

Human *M-* and *L-opsin* mRNA transcripts exhibit ~98% sequence identity[1,37,38], which complicates expression analysis. We quantified *M-* and *L-opsin* expression in RNA-seq datasets by analyzing pileup counts, quantifying the total number of reads supporting M- versus L-opsin at 20 divergent nucleotides (**Fig. 1B**), and normalizing by the total number of reads aligned to these divergent sites.

We first tested this computational approach with the Weri-Rb-1 retinoblastoma cell line, which expresses *M-* and *L-opsins* at low levels[39]. T3, the active form of thyroid hormone, induces *M-* and *L-opsin* expression in Weri-Rb-1 cells[36,40]. We conducted RNA-seq and observed an increase in both *M-* and *L-opsin* in T3-treated Weri-Rb-1 cells compared to untreated cells (**Fig. S1A-B**), validating our approach to quantify *M-* and *L-opsin* expression.

113 We assessed the timing of *M-* and *L-opsin* expression during human retinal
114 development by analyzing published RNA-seq data[41]. The recent availability of these data
115 and the challenges in attaining fetal retinal samples likely prevented this type of analysis
116 previously. We assessed expression in 12 samples from prenatal day 52/54 through day
117 136 postconception. *M-opsin* was strongly expressed from day 115 through day 136 (**Fig.**
118 **1C**). In contrast, minimal *L-opsin* expression was observed through day 136 (**Fig. 1C**).
119 We analyzed three independent adult human retinal samples from a published dataset[42]
120 and observed expression of *M-* and *L-opsin* (**Fig. 1D**). These data suggest that *M-opsin*
121 is expressed before *L-opsin* during human retinal development.
122

123 **Natural variation in L:M cone ratios implicates retinoic acid signaling**

124 We next sought to identify a regulatory mechanism controlling specification of M
125 and L cones. L:M cone ratios vary widely among people with normal color vision, ranging
126 from 6% to 94% L cones[21,25,43-46]. We hypothesized that DNA sequence differences in the
127 *L/M-opsin* gene locus or putative regulatory genes influence variation in L:M cone
128 ratios[47,48]. We assessed L:M cone ratios from 738 males with normal color vision using
129 the flicker-photometric electroretinogram (FP-ERG). We focused our study on males
130 because variation at the X-linked *L/M-opsin* gene locus is a primary site for mutations
131 causing red-green color blindness, and an increase in variation could be revealed in
132 hemizygous conditions[49-52]. In this population, we observed ratios ranging from 15% to
133 110% L cones (**Fig. 2A**). The association between FP-ERG and % L is nonlinear and as
134 100% is approached, very small changes in measured spectral sensitivities are
135 associated with relatively large changes in estimates of % L. Thus, near 100%, small

136 experimental errors led to some values that exceeded 100% upon normalization.

137 To identify the genetic basis of this variation, we performed an association study
138 using the L:M cone ratio data and the targeted DNA sequencing of 21 gene regions,
139 including the *L/M-opsin* gene locus (*OPN1LW/MW*), the *S-opsin* gene (*OPN1SW*), and
140 regulatory genes with putative roles in cone subtype specification including *DIO1*, *PIAS3*,
141 *RXRG*, *OTX1*, *NEUROD1*, *THRB*, *NR2F1/COUP-TFI*, *RORB*, *CYP26A1/C1*, *NRL*, *OTX2*,
142 *DIO2*, *DIO3*, *ONECUT1*, *NR2E3*, *NR2F2/COUP-TFII*, *RARA*, *ONECUT2*, and *SALL3*
143 (**Fig. S2**).

144 For each of the 21 gene regions, we isolated DNA for each gene of interest by
145 targeting sequence intervals delineated by the end coordinate of the neighboring
146 upstream gene to the start coordinate of the neighboring downstream gene using an
147 oligo-based pull-down method (**Fig. S2**). If the neighboring upstream or downstream
148 genes were less than 100 kb from the gene of interest, we expanded the pulled down
149 region to include at least 100 kb of upstream and downstream sequence (**Fig. S2**). We
150 generated custom-designed oligos and used a solution-based capture method for target
151 enrichment based on the Roche Nimble Design software. We barcoded and pooled
152 samples, which we sequenced with 125 bp paired-end reads. We mapped the reads,
153 genotyped the samples, and evaluated associations with L:M ratios (**Fig. 2C**).

154 From this approach, we identified a significant association between SNP
155 rs372754794 ($\hat{\beta}$ = -18.54, p-value = 1.67×10^{-5}, R^2 = 0.0569) and variation in L:M cone
156 ratio (**Fig. 2B-C**). This SNP, which occurs within the targeted sequence spanning
157 *NR2F2/COUP-TFII,* lies in a non-coding RNA immediately upstream of *NR2F2* (**Fig. 2D**).
158 The minor (G) allele, which is associated with reduced L:M ratio, was nearly exclusive to

159 African American (and few African) subjects within our sample (MAF = 0. 0359; **Fig. S3A**)
160 and exhibited similar patterns of frequency differentiation in external data from the 1000
161 Genomes Project. We note that the association with L:M ratio was robust even when
162 restricting analysis to African American subjects ($\hat{\beta}$ = -14.45, p-value = 1.44×10^{-4}, R^2 =
163 0.1052), arguing against ancestry as a confounding factor (**Fig. S3B**). Within African
164 American populations from the 1000 Genomes Project[53], rs372754794 exhibited only
165 modest linkage disequilibrium (LD) with other nearby variants (**Fig. S3C**), such that the
166 associated haplotype is confined to the *NR2F2-AS1* transcript.

167 NR2F2 is a nuclear receptor that mediates RA signaling[54]. While studying bilateral
168 symmetry in the vertebrate body plan, Vilhais-Neto and colleagues showed that Nr2f2
169 binding was enriched at a retinoic acid response element (RARE) and that Nr2f2
170 knockdown led to a reduction in RARE activity. Nr2f2 was also found at the *Rarb*
171 promoter, a well-characterized RA target gene, and its recruitment increased in the
172 presence of RA. Nr2f2 forms a complex with a retinoic acid receptor (Rar), Rere, and
173 p300, and the recruitment of Rar, Rere, and p300 at the *Rarb* promoter is dependent on
174 Nr2f2[55]. Similarly, Litchfield and colleagues showed that RA increased NR2F2 binding to
175 a RARE in *RARB2*, an RA target gene. RA-mediated activation of *Rarβ2* was dependent
176 on NR2F2[56]. NR2F2 mediates RA signaling in other contexts including lung
177 morphogenesis[57], trans-differentiation of breast cancer cells[58], and metabolism in
178 hepatocytes[59]. NR2F2 also bound RAREs in the PEPCK[60] and Gck gene promoters[59].
179 Additionally, RA increases NR2F2 expression[56,61]. NR2F2 can be activated by high, likely
180 nonphysiological, levels of RA[62]. These studies support a role for NR2F2 in regulating
181 target genes in the RA signaling pathway.

182 The second strongest associated SNP (rs36102671), which did not achieve
183 statistical significance upon multiple testing correction (Bonferroni correction p-value
184 threshold = 1.73×10^{-5}), lies within the first intron of the *RARA* gene, which encodes a
185 receptor for RA (**Fig. 2C**). The minor (A) allele, which segregates at low allele frequencies
186 in globally diverse populations (**Fig. S3D**), is associated with decreased L:M ratio ($\hat{\beta}$ = -
187 15.95, p-value = 6.54×10^{-5}). Within European populations, LD at this locus extends over
188 an ~200 Kb region of chromosome 17, including *RARA* itself, as well as *MSL1*, *CASC3*,
189 *MIR6866*, *MIR6867*, *RAPGEFL1*, *WIPF2*, and *CDC6* (R^2 > 0.7). In external data from the
190 Genotype Tissue Expression Project (GTEx), the SNP also exhibits an association with
191 altered splicing of RARA based on RNA sequencing of whole blood (**Fig. S3E**)[63].
192 While validation and further dissection of these association results requires
193 investigation in a larger cohort, the consistent appearance of RA-related candidates
194 pointed to a potential role for RA signaling in the specification of M and L cone subtypes
195 in humans.
196
197 **RA-synthesis genes are highly expressed early and decrease during development**
198 Considering the association between M/L cone ratios and the natural variant in
199 NR2F2, we analyzed a published dataset[41] to assess expression of RA pathway genes
200 during early human retinal development. The nuclear receptor genes *NR2F2* and *RARA*
201 are expressed at consistent levels (**Fig. 2E, S3F**). Aldehyde Dehydrogenases (ALDHs)
202 convert retinaldehyde to synthesize RA. *ALDH1A1* and *ALDH1A3* are expressed early in
203 development and decrease over time, whereas *ALDH1A2* is expressed at very low levels
204 (**Fig. 2F**). CYP26 enzymes catalyze the degradation of RA. *CYP26A1* is steadily

205 expressed, whereas *CYP26B1* and *CYP26C1* are not expressed (**Fig. 2G**). The high
206 expression of two RA-synthesis enzymes early and the consistent expression of receptors
207 and RA-degradatory enzymes suggested that RA signaling is high early and decreases
208 during retinal development. Coupled with the observation that *M-opsin* is expressed
209 before *L-opsin*, we hypothesized that high RA signaling early promotes M cone fate and
210 suppresses L cone fate.
211

212 **Visualization of *M-* and *L-opsin* expression**

213 To test the role of RA signaling, we first needed to develop a method to visualize
214 *M-* and *L-opsin* mRNA expression and observe M and L cones in human retinal and
215 organoid tissue. The opsin protein sequences are ~96% identical and the cDNA
216 sequences are ~98% identical, preventing the generation of antibodies and large
217 fragment *in situ* hybridization reagents that distinguish *M-* and *L-opsin* expression *in*
218 *vivo*[64].

219 To directly visualize *M-* and *L-opsin* expression in fixed retinas and organoids, we
220 designed an oligo-based *in situ* hybridization approach. We generated a 40-nucleotide
221 duplex probe for *M-opsin* and a 42-nucleotide duplex probe for *L-opsin* with partial overlap
222 that target a region with 3 differential nucleotides in the *M-* and *L-opsin* mRNAs (**Fig. 1B,**
223 **3A**). We utilized colorimetric *in situ* hybridization to visualize *M-opsin* in blue and *L-opsin*
224 in red.

225 We next tested the specificity of this approach to distinguish *M-* and *L-opsin*
226 mRNA. HEK293 cells transfected with no plasmid showed no expression (**Fig. 3B, S4**).
227 Cells transfected with *M-opsin* cDNA showed expression of *M-opsin* but not *L-opsin* (**Fig.**

228 **3C, S4**). Cells transfected with *L-opsin* cDNA displayed expression of *L-opsin* but not *M-*
229 *opsin* (**Fig. 3D, S4**). Cells transfected with either *M-opsin* cDNA or *L-opsin* cDNA and
230 then mixed into a single sample showed individual expression of *M-opsin* only or *L-opsin*
231 only (**Fig. 3E, S4**). Finally, cells co-transfected with both *M-opsin* and *L-opsin* cDNA
232 displayed co-expression of both *M-* and *L-opsin* (**Fig. 3F, S4**). Therefore, this *in situ*
233 hybridization method distinguishes between the highly similar *M-* and *L-opsin* mRNAs in
234 cultured cells.

235 We tested this approach in sectioned, flash-frozen adult human retinas. We
236 observed exclusive expression of *M-* and *L-opsins* in individual cones (**Fig. 3G**). Thus,
237 this *in situ* hybridization method unambiguously distinguishes *M-* and *L-opsin* mRNA.

238

239 **RA promotes M cones and suppresses L cones early in human retinal organoids**

240 We next sought to test our hypothesis that high RA signaling early promotes M
241 cone fate and suppresses L cone fate in human retinal organoids. Differentiation of
242 human retinal organoids involves addition of all-trans RA (hereafter referred to as RA) on
243 days 20-43 to promote early retinal patterning (**Fig. S5**). RA was not added from day 43
244 to day 200, a timeframe which includes the end of primitive retina differentiation and the
245 complete duration of cell fate specification (**'No RA'**).

246 We first used our *in situ* hybridization approach to examine the timing of M and L
247 cone generation during human retinal organoid development. At day 120, we observed
248 very few M and L cones (**Fig. 4A, S6A**). We first observed significant numbers of M and
249 L cones on day 140 (**Fig. 4A, S6A**). From day 140 through day 200, organoids were
250 enriched for L cones (**Fig. 4A-B, S6A**). These observations suggested that human retinal

251 organoids differentiated with this protocol are missing developmental cues to generate
252 large populations of M cones before L cones as in human fetal development.

253 To test whether addition of RA induced M cone generation in retinal organoids, we
254 added 1.0 μM RA over different timeframes and assessed M and L cones at day 200 (**Fig.**
255 **4C**). Organoids grown in supplemental RA throughout development failed to differentiate,
256 yielding minimal M or L cones (N=6). Addition of RA early in development from days 43
257 to 130 yielded organoids with almost exclusively M cones at day 200 (98.35% M, 1.65%
258 L, 0% co-expressing; **Fig. 4D-E; 'Early RA'**). To corroborate this observation, we
259 conducted RNA-seq on ESC-derived organoids grown in 'Early RA' conditions and
260 observed high *M-opsin* and minimal *L-opsin* expression (**Fig. S1C**). We also analyzed our
261 previously published RNA-seq data on iPSC-derived organoids grown in 'Early RA'
262 conditions and observed near exclusive expression of *M-opsin* (**Fig. S1D**). Addition of RA
263 late in development from days 130 to 200 yielded L cone-enriched organoids at day 200
264 (6.35% M, 92.56% L, 1.10% co-expressing; **Fig. 4D-E; 'Late RA'**), similar to organoids
265 grown with no additional RA. We observed no significant differences in overall M/L cone
266 densities at day 200 across experimental conditions (**Fig. S6B**). Together, these data
267 suggest that RA is sufficient to induce M cones and suppress L cones early in retinal
268 organoid development.

269

270 **Discussion**

271 We investigated the regulation of M and L cone subtype specification in the human
272 retina. Our gene expression analysis suggested that *M-opsin* is expressed before *L-opsin*
273 in human retinas. Our association study implicated a role for RA signaling in M versus L

274 cone subtype specification. ALDH genes, which code for RA synthesis proteins, are highly
275 expressed early in retinal development and then decrease over time, suggesting that RA
276 signaling is high early and decreases during retinal development. Human retinal
277 organoids are L cone-rich in the absence of supplemental RA. RA is sufficient to induce
278 M cones and suppress L cones early in organoid development. Our data support the
279 temporal specification of M cones followed by L cones and a role for RA signaling early
280 to promote M cones and suppress L cones (**Fig. 4F-G**).

281 The main models for M and L cone subtype specification involved stochastic and
282 temporal mechanisms[1,13,20-23,25,27,33]. Previously, reporter constructs testing regions of the
283 *L/M-opsin* gene locus in the mouse retina suggested that the distance and order of the
284 *L/M-opsin* promoters to the LCR determined the frequency of expression[13]. These results
285 supported a model that cone specification was controlled by a stochastic mechanism in
286 which the LCR randomly loops to the *M-opsin* or *L-opsin* promoter to determine
287 expression state and cone subtype[13]. The temporal model was based on geographic
288 distributions of M and L cones in the human retina, with higher proportions of L cones in
289 the late-developing peripheral retina compared to the early-developing central retina[21-33].
290 Our studies provide direct experimental evidence for the temporality of M and L cone
291 generation and show that RA signaling regulates this mechanism. We speculate that
292 temporal regulation by RA signaling is a main developmental driver that acts in
293 conjunction with stochasticity in gene regulation to specify cone subtypes.

294 Our observations suggest that RA signaling influences cone fates before the
295 expression of *M-* and *L-opsin* mRNA. In human retinal organoids, *M-* and *L-opsin* mRNA
296 expression is first observed by day 140 (**Fig. 4A, S1D**), whereas addition of RA before

297 day 130 induces M cones and suppresses L cones (**Fig. 4D**). In human fetal retinas, *M-*
298 *opsin* mRNA expression is readily observed on day 115 (**Fig. 1C**), whereas expression
299 of RA synthesis genes (i.e. ALDHs) is highest on days 53 and 57 and then decreases
300 (**Fig. 2F**). RA signaling may act at the gene locus to regulate opsin expression directly or
301 function upstream to influence M and L cone fates.

302 Temporal regulation of RA signaling is important for the differentiation of
303 photoreceptors during retinal development in a variety of species[65-68]. The arrangement
304 of the LCR regulatory element and *L-* and *M-opsin* genes in humans resembles an
305 independently evolved opsin gene array in zebrafish[69]. In zebrafish, a regulatory element
306 called the locus activating region (LAR) lies upstream of the *opn1lw1* and *opn1lw2* opsin
307 genes[70]. Expression of these two long-wavelength-detecting opsins defines cone
308 subtypes: LWS1 cones express *opn1lw1* and LWS2 cones express *opn1lw2*.
309 Specification of these two cone subtypes is temporally distinct, with *opn1lw2* expressed
310 first during embryogenesis and *opn1lw1* expressed later after hatching. This temporal
311 switch is controlled by retinoic acid (RA) signaling, which promotes *opn1lw1* and inhibits
312 *opn1lw2* late in development[71]. This late role for RA signaling in promoting expression of
313 the proximal opsin in zebrafish contrasts with our findings that RA signaling functions
314 early to promote expression of the distal opsin in humans. These observations suggest
315 differences in evolution of both the regulation of RA signaling and the *cis*-regulatory logic
316 controlling opsin expression in these species.

317 Studying primate development poses specific challenges including limited access
318 to tissue, a lack of a controlled genetic background, and an inability to genetically or
319 pharmacologically manipulate developing retinal tissue. Commonly used vertebrate

model organisms such as mice, fish, and chickens have provided numerous insights into cell fate specification during vertebrate retinal development. However, differences between these systems and the primate visual system prevent interrogation of questions that can only be addressed in developing human tissue. Our studies show that human retinal organoids are a powerful model system to investigate developmental processes that are unique to humans and Old World monkeys.

Funding

S.E.H. was an F31 Ruth L. Kirschstein NRSA Fellow and supported by the National Eye Institute under grant 5F31EY029157-02. K.C.E. was a Howard Hughes Medical Institute Gilliam Fellow and was supported by the National Science Foundation Graduate Research Fellowship Program under grant 1746891. K.A.H. was supported by the National Science Foundation Graduate Research Fellowship Program under grant 1746891. R.C.M. was supported by R35GM133747 from NIH/NIGMS. M.N. and J.N. were supported by NEI grants R01EY021242 and P30EY001730, and unrestricted funds from Research to Prevent Blindness to ophthalmology at UW. R.J.J. was supported by the National Eye Institute R01EY030872 and the BrightFocus foundation G2019300.

338 **References**

339 1 Nathans, J., Thomas, D. & Hogness, D. S. Molecular genetics of human color
340 vision: the genes encoding blue, green, and red pigments. *Science* **232**, 193-202,
341 doi:10.1126/science.2937147 (1986).

342 2 Yokoyama, S. & Radlwimmer, F. B. The "five-sites" rule and the evolution of red
343 and green color vision in mammals. *Mol Biol Evol* **15**, 560-567,
344 doi:10.1093/oxfordjournals.molbev.a025956 (1998).

345 3 Vollrath, D., Nathans, J. & Davis, R. W. Tandem array of human visual pigment
346 genes at Xq28. *Science* **240**, 1669-1672, doi:10.1126/science.2837827 (1988).

347 4 Dulai, K. S., von Dornum, M., Mollon, J. D. & Hunt, D. M. The evolution of
348 trichromatic color vision by opsin gene duplication in New World and Old World
349 primates. *Genome Res* **9**, 629-638 (1999).

350 5 Jacobs, G. H. & Neitz, J. Color vision in squirrel monkeys: sex-related differences
351 suggest the mode of inheritance. *Vision Res* **25**, 141-143, doi:10.1016/0042-
352 6989(85)90088-4 (1985).

353 6 Mollon, J. D., Bowmaker, J. K. & Jacobs, G. H. Variations of colour vision in a New
354 World primate can be explained by polymorphism of retinal photopigments. *Proc*
355 *R Soc Lond B Biol Sci* **222**, 373-399, doi:10.1098/rspb.1984.0071 (1984).

356 7 Onishi, A. *et al.* Dichromatism in macaque monkeys. *Nature* **402**, 139-140,
357 doi:10.1038/45966 (1999).

358 8 Onishi, A. *et al.* Variations in long- and middle-wavelength-sensitive opsin gene
359 loci in crab-eating monkeys. *Vision Res* **42**, 281-292, doi:10.1016/s0042-
360 6989(01)00293-0 (2002).

361 9 Yamaguchi, T., Motulsky, A. G. & Deeb, S. S. Visual pigment gene structure and
362 expression in human retinae. *Hum Mol Genet* **6**, 981-990,
363 doi:10.1093/hmg/6.7.981 (1997).
364 10 Peng, Y. R. *et al.* Molecular Classification and Comparative Taxonomics of Foveal
365 and Peripheral Cells in Primate Retina. *Cell* **176**, 1222-1237 e1222,
366 doi:10.1016/j.cell.2019.01.004 (2019).
367 11 Hagstrom, S. A., Neitz, M. & Neitz, J. Cone pigment gene expression in individual
368 photoreceptors and the chromatic topography of the retina. *J Opt Soc Am A Opt*
369 *Image Sci Vis* **17**, 527-537, doi:10.1364/josaa.17.000527 (2000).
370 12 Winderickx, J., Battisti, L., Motulsky, A. G. & Deeb, S. S. Selective expression of
371 human X chromosome-linked green opsin genes. *Proc Natl Acad Sci U S A* **89**,
372 9710-9714, doi:10.1073/pnas.89.20.9710 (1992).
373 13 Smallwood, P. M., Wang, Y. & Nathans, J. Role of a locus control region in the
374 mutually exclusive expression of human red and green cone pigment genes. *Proc*
375 *Natl Acad Sci U S A* **99**, 1008-1011, doi:10.1073/pnas.022629799 (2002).
376 14 Wang, Y. *et al.* A locus control region adjacent to the human red and green visual
377 pigment genes. *Neuron* **9**, 429-440, doi:10.1016/0896-6273(92)90181-c (1992).
378 15 Drummond-Borg, M., Deeb, S. S. & Motulsky, A. G. Molecular patterns of X
379 chromosome-linked color vision genes among 134 men of European ancestry.
380 *Proc Natl Acad Sci U S A* **86**, 983-987, doi:10.1073/pnas.86.3.983 (1989).
381 16 Neitz, M., Bollinger, K. & Neitz, J. in *Normal and defective colour vision* (eds J.
382 D. Mollon, Joel Pokorny, & K. Knoblauch) 318-327 (Oxford University Press,
383 2003).

384 17 Winderickx, J. *et al.* Defective colour vision associated with a missense mutation
385 in the human green visual pigment gene. *Nat Genet* **1**, 251-256,
386 doi:10.1038/ng0792-251 (1992).
387 18 Hayashi, T., Motulsky, A. G. & Deeb, S. S. Position of a 'green-red' hybrid gene in
388 the visual pigment array determines colour-vision phenotype. *Nat Genet* **22**, 90-
389 93, doi:10.1038/8798 (1999).
390 19 Bollinger, K., Sjoberg, S. A., Neitz, M. & Neitz, J. Topographical cone
391 photopigment gene expression in deutan-type red-green color vision defects.
392 *Vision Res* **44**, 135-145, doi:10.1016/j.visres.2003.09.006 (2004).
393 20 Wang, Y. *et al.* Mutually exclusive expression of human red and green visual
394 pigment-reporter transgenes occurs at high frequency in murine cone
395 photoreceptors. *Proc Natl Acad Sci U S A* **96**, 5251-5256,
396 doi:10.1073/pnas.96.9.5251 (1999).
397 21 Hagstrom, S. A., Neitz, J. & Neitz, M. Variations in cone populations for red-green
398 color vision examined by analysis of mRNA. *Neuroreport* **9**, 1963-1967,
399 doi:10.1097/00001756-199806220-00009 (1998).
400 22 Neitz, M., Balding, S. D., McMahon, C., Sjoberg, S. A. & Neitz, J. Topography of
401 long- and middle-wavelength sensitive cone opsin gene expression in human and
402 Old World monkey retina. *Vis Neurosci* **23**, 379-385,
403 doi:10.1017/S095252380623325X (2006).
404 23 Bowmaker, J. K., Parry, J. W. L., and Mollon, J.D. The arrangement of L and M
405 cones in human and a primate retina. *Normal and defective colour vision*, 39-50
406 (2003).

24 Bumsted, K. & Hendrickson, A. Distribution and development of short-wavelength cones differ between Macaca monkey and human fovea. *J Comp Neurol* **403**, 502-516 (1999).

25 Carroll, J., Neitz, J. & Neitz, M. Estimates of L:M cone ratio from ERG flicker photometry and genetics. *J Vis* **2**, 531-542, doi:10.1167/2.8.1 (2002).

26 Cornish, E. E., Xiao, M., Yang, Z., Provis, J. M. & Hendrickson, A. E. The role of opsin expression and apoptosis in determination of cone types in human retina. *Exp Eye Res* **78**, 1143-1154, doi:10.1016/j.exer.2004.01.004 (2004).

27 Kuchenbecker, J. A., Sahay, M., Tait, D. M., Neitz, M. & Neitz, J. Topography of the long- to middle-wavelength sensitive cone ratio in the human retina assessed with a wide-field color multifocal electroretinogram. *Vis Neurosci* **25**, 301-306, doi:10.1017/S0952523808080474 (2008).

28 La Vail, M. M., Rapaport, D. H. & Rakic, P. Cytogenesis in the monkey retina. *J Comp Neurol* **309**, 86-114, doi:10.1002/cne.903090107 (1991).

29 Martin, P. R., Grunert, U., Chan, T. L. & Bumsted, K. Spatial order in short-wavelength-sensitive cone photoreceptors: a comparative study of the primate retina. *J Opt Soc Am A Opt Image Sci Vis* **17**, 557-567, doi:10.1364/josaa.17.000557 (2000).

30 Mollon, J. D. & Bowmaker, J. K. The spatial arrangement of cones in the primate fovea. *Nature* **360**, 677-679, doi:10.1038/360677a0 (1992).

31 Otake, S., Gowdy, P. D. & Cicerone, C. M. The spatial arrangement of L and M cones in the peripheral human retina. *Vision Res* **40**, 677-693, doi:10.1016/s0042-6989(99)00202-3 (2000).

430 32 Roorda, A., Metha, A. B., Lennie, P. & Williams, D. R. Packing arrangement of the
431 three cone classes in primate retina. *Vision Res* **41**, 1291-1306,
432 doi:10.1016/s0042-6989(01)00043-8 (2001).
433 33 Xiao, M. & Hendrickson, A. Spatial and temporal expression of short, long/medium,
434 or both opsins in human fetal cones. *J Comp Neurol* **425**, 545-559 (2000).
435 34 Nakano, T. *et al.* Self-formation of optic cups and storable stratified neural retina
436 from human ESCs. *Cell Stem Cell* **10**, 771-785, doi:10.1016/j.stem.2012.05.009
437 (2012).
438 35 Wahlin, K. J. *et al.* Photoreceptor Outer Segment-like Structures in Long-Term 3D
439 Retinas from Human Pluripotent Stem Cells. *Sci Rep* **7**, 766, doi:10.1038/s41598-
440 017-00774-9 (2017).
441 36 Eldred, K. C. *et al.* Thyroid hormone signaling specifies cone subtypes in human
442 retinal organoids. *Science* **362**, doi:10.1126/science.aau6348 (2018).
443 37 Neitz, J. & Neitz, M. The genetics of normal and defective color vision. *Vision Res*
444 **51**, 633-651, doi:10.1016/j.visres.2010.12.002 (2011).
445 38 Verrelli, B. C. & Tishkoff, S. A. Signatures of selection and gene conversion
446 associated with human color vision variation. *Am J Hum Genet* **75**, 363-375,
447 doi:10.1086/423287 (2004).
448 39 Shaaban, S. A. & Deeb, S. S. Functional analysis of the promoters of the human
449 red and green visual pigment genes. *Invest Ophthalmol Vis Sci* **39**, 885-896
450 (1998).

451 40 Liu, Y., Fu, L., Chen, D. G. & Deeb, S. S. Identification of novel retinal target genes
452 of thyroid hormone in the human WERI cells by expression microarray analysis.
453 *Vision Res* **47**, 2314-2326, doi:10.1016/j.visres.2007.04.023 (2007).
454 41 Hoshino, A. *et al.* Molecular Anatomy of the Developing Human Retina. *Dev Cell*
455 **43**, 763-779 e764, doi:10.1016/j.devcel.2017.10.029 (2017).
456 42 Pinelli, M. *et al.* An atlas of gene expression and gene co-regulation in the human
457 retina. *Nucleic Acids Res* **44**, 5773-5784, doi:10.1093/nar/gkw486 (2016).
458 43 Dartnall, H. J., Bowmaker, J. K. & Mollon, J. D. Human visual pigments:
459 microspectrophotometric results from the eyes of seven persons. *Proc R Soc Lond*
460 *B Biol Sci* **220**, 115-130, doi:10.1098/rspb.1983.0091 (1983).
461 44 Hofer, H., Carroll, J., Neitz, J., Neitz, M. & Williams, D. R. Organization of the
462 human trichromatic cone mosaic. *J Neurosci* **25**, 9669-9679,
463 doi:10.1523/JNEUROSCI.2414-05.2005 (2005).
464 45 McMahon, C., Carroll, J., Awua, S., Neitz, J. & Neitz, M. The L:M cone ratio in
465 males of African descent with normal color vision. *J Vis* **8**, 5 1-9, doi:10.1167/8.2.5
466 (2008).
467 46 Roorda, A. & Williams, D. R. The arrangement of the three cone classes in the
468 living human eye. *Nature* **397**, 520-522, doi:10.1038/17383 (1999).
469 47 McMahon, C., Neitz, J. & Neitz, M. Evaluating the human X-chromosome pigment
470 gene promoter sequences as predictors of L:M cone ratio variation. *J Vis* **4**, 203-
471 208, doi:10.1167/4.3.7 (2004).

472 48 Gunther, K. L., Neitz, J. & Neitz, M. Nucleotide polymorphisms upstream of the X-
473 chromosome opsin gene array tune L:M cone ratio. *Vis Neurosci* **25**, 265-271,
474 doi:10.1017/S0952523808080280 (2008).
475 49 Neitz, J. & Jacobs, G. H. Polymorphism of the long-wavelength cone in normal
476 human colour vision. *Nature* **323**, 623-625, doi:10.1038/323623a0 (1986).
477 50 Nathans, J. *et al.* Molecular genetics of human blue cone monochromacy. *Science*
478 **245**, 831-838, doi:10.1126/science.2788922 (1989).
479 51 Nathans, J., Piantanida, T. P., Eddy, R. L., Shows, T. B. & Hogness, D. S.
480 Molecular genetics of inherited variation in human color vision. *Science* **232**, 203-
481 210, doi:10.1126/science.3485310 (1986).
482 52 Merbs, S. L. & Nathans, J. Absorption spectra of the hybrid pigments responsible
483 for anomalous color vision. *Science* **258**, 464-466, doi:10.1126/science.1411542
484 (1992).
485 53 Genomes Project, C. *et al.* A global reference for human genetic variation. *Nature*
486 **526**, 68-74, doi:10.1038/nature15393 (2015).
487 54 Zhang, R., Wang, Y., Li, R. & Chen, G. Transcriptional Factors Mediating Retinoic
488 Acid Signals in the Control of Energy Metabolism. *Int J Mol Sci* **16**, 14210-14244,
489 doi:10.3390/ijms160614210 (2015).
490 55 Vilhais-Neto, G. C. *et al.* Rere controls retinoic acid signalling and somite bilateral
491 symmetry. *Nature* **463**, 953-957, doi:10.1038/nature08763 (2010).
492 56 Litchfield, L. M. *et al.* Identification and characterization of nucleolin as a COUP-
493 TFII coactivator of retinoic acid receptor beta transcription in breast cancer cells.
494 *PLoS One* **7**, e38278, doi:10.1371/journal.pone.0038278 (2012).

495 57 Malpel, S., Mendelsohn, C. & Cardoso, W. V. Regulation of retinoic acid signaling
496 during lung morphogenesis. *Development* **127**, 3057-3067 (2000).
497 58 Prahalad, P., Dakshanamurthy, S., Ressom, H. & Byers, S. W. Retinoic acid
498 mediates regulation of network formation by COUP-TFII and VE-cadherin
499 expression by TGFbeta receptor kinase in breast cancer cells. *PLoS One* **5**,
500 e10023, doi:10.1371/journal.pone.0010023 (2010).
501 59 Li, R. *et al.* A RARE of hepatic Gck promoter interacts with RARalpha, HNF4alpha
502 and COUP-TFII that affect retinoic acid- and insulin-induced Gck expression. *J*
503 *Nutr Biochem* **25**, 964-976, doi:10.1016/j.jnutbio.2014.04.009 (2014).
504 60 Scribner, K. B., Odom, D. P. & McGrane, M. M. Nuclear receptor binding to the
505 retinoic acid response elements of the phosphoenolpyruvate carboxykinase gene
506 in vivo: effects of vitamin A deficiency. *J Nutr Biochem* **18**, 206-214,
507 doi:10.1016/j.jnutbio.2006.03.011 (2007).
508 61 Achatz, G. *et al.* Functional domains of the human orphan receptor ARP-1/COUP-
509 TFII involved in active repression and transrepression. *Mol Cell Biol* **17**, 4914-
510 4932, doi:10.1128/mcb.17.9.4914 (1997).
511 62 Kruse, S. W. *et al.* Identification of COUP-TFII orphan nuclear receptor as a
512 retinoic acid-activated receptor. *PLoS Biol* **6**, e227,
513 doi:10.1371/journal.pbio.0060227 (2008).
514 63 Consortium, G. T. The GTEx Consortium atlas of genetic regulatory effects across
515 human tissues. *Science* **369**, 1318-1330, doi:10.1126/science.aaz1776 (2020).
516 64 Pettan-Brewer, C., Fu, L. & Deeb, S. S. Distinguishing L from M photopigment
517 coding sequences by hybridization to novel locked nucleic acid (LNA)

518 oligonucleotide probes. *Vis Neurosci* **25**, 283-287,
519 doi:10.1017/S0952523808080607 (2008).
520 65 Sen, J., Harpavat, S., Peters, M. A. & Cepko, C. L. Retinoic acid regulates the
521 expression of dorsoventral topographic guidance molecules in the chick retina.
522 *Development* **132**, 5147-5159, doi:10.1242/dev.02100 (2005).
523 66 Hyatt, G. A., Schmitt, E. A., Marsh-Armstrong, N. R. & Dowling, J. E. Retinoic acid-
524 induced duplication of the zebrafish retina. *Proc Natl Acad Sci U S A* **89**, 8293-
525 8297, doi:10.1073/pnas.89.17.8293 (1992).
526 67 Wilson, J. G., Roth, C. B. & Warkany, J. An analysis of the syndrome of
527 malformations induced by maternal vitamin A deficiency. Effects of restoration of
528 vitamin A at various times during gestation. *Am J Anat* **92**, 189-217,
529 doi:10.1002/aja.1000920202 (1953).
530 68 da Silva, S. & Cepko, C. L. Fgf8 Expression and Degradation of Retinoic Acid Are
531 Required for Patterning a High-Acuity Area in the Retina. *Dev Cell* **42**, 68-81 e66,
532 doi:10.1016/j.devcel.2017.05.024 (2017).
533 69 Chinen, A., Hamaoka, T., Yamada, Y. & Kawamura, S. Gene duplication and
534 spectral diversification of cone visual pigments of zebrafish. *Genetics* **163**, 663-
535 675 (2003).
536 70 Tsujimura, T., Hosoya, T. & Kawamura, S. A single enhancer regulating the
537 differential expression of duplicated red-sensitive opsin genes in zebrafish. *PLoS*
538 *Genet* **6**, e1001245, doi:10.1371/journal.pgen.1001245 (2010).

539 71 Mitchell, D. M. *et al.* Retinoic Acid Signaling Regulates Differential Expression of
540 the Tandemly-Duplicated Long Wavelength-Sensitive Cone Opsin Genes in
541 Zebrafish. *PLoS Genet* **11**, e1005483, doi:10.1371/journal.pgen.1005483 (2015).
542
543

544 **Materials and Methods**

545

546 **Cell line maintenance**

547 H7 ESC (WA07, WiCell) and episomal-derived EP1.1 iPSC were used for retinal
548 organoid differentiation. Pluripotency of EP1.1 cells was evaluated previously with
549 antibodies for NANOG, OCT4, SOX2, and SSEA2[1]. Stem cells were maintained in
550 mTeSR™1 (85857, Stem Cell Technologies) on 1% (v/v) Matrigel-GFR™ (354230, BD
551 Biosciences) coated dishes and grown at 37ºC in a HERAcell 150i or 160i 10% CO_2 and
552 5% O_2 incubator (Thermo Fisher Scientific). Cells were passaged every 4-5 days
553 according to confluence as in Wahlin *et. al*[1]. Cells were passaged with Accutase
554 (SCR005, Sigma) for 7-12 minutes to be dissociated to single cells. Cells in Accutase
555 were added 1:2 to mTeSR™1 plus 5 μM Blebbistatin (Bleb, B0560, Sigma), pelleted at
556 150g for 5 minutes, and suspended in mTeSR™1 plus Bleb and plated at 5,000-15,000
557 cells per well in a 6-well plate. Cells were fed with mTeSR™1 48 hours following
558 passage and every 24 hours until passaged again. To minimize cell stress, no
559 antibiotics were used.

560 Weri-Rb-1 retinoblastoma cells were obtained from ATCC and maintained in
561 RPMI 1640 Medium (11875135,Gibco) + 10% Fetal Bovine Serum (16140071, Gibco) +
562 1X Penicillin-Streptomycin (30-002-CI, Corning) at 37ºC in a HERAcell 150i or 160i 5%
563 CO_2 incubator (Thermo Fisher Scientific). Cells were passaged every 4 days at ~1×10^5
564 – 2×10^6 cells/mL in uncoated flasks by pelleting at 150g for 5 minutes and
565 resuspending in fresh media.

566 HEK293 cells were a gift from the Kuruvilla lab at Johns Hopkins University. Cells
567 were maintained in DMEM 4.5 g/L D-glucose, L-glutamine (11965084, Gibco) + 10%
568 Fetal Bovine Serum (16140071, Gibco) + 1X Penicillin-Streptomycin (30-002-CI,
569 Corning) at 37ºC in a HERAcell 150i or 160i 5% CO_2 incubator (Thermo Fisher
570 Scientific). Cells were split 1:4 – 1:10 every 2-3 days when approximately 80% confluent
571 and kept in 6-well dishes or uncoated flasks using Trypsin (0.25%)-EDTA (0.02%) in
572 HBSS (118-093-721, Quality Biological).
573 Cell lines were tested monthly for mycoplasma using MycoAlert (LT07, Lonza).
574
575 **Cell Culture Media**
576 **Stem Cell media:** mTeSR1 (85857, StemCell Technologies)
577 **E6 supplement**: 970 μg/mL Insulin (11376497001, Roche), 535 μg/mL holo-
578 transferrin (T0665, Sigma), 3.20 mg/mL L-ascorbic acid (A8960, Sigma), 0.7 μg/mL
579 sodium selenite (S5261, Sigma).
580 **BE6.2 media for early retinal differentiation**: 2.5% E6 supplement (above), 2%
581 B27 Supplement (50X) minus Vitamin A (12587010, Gibco), 1% Glutamax (35050061,
582 Gibco), 1% NEAA (11140050, Gibco), 1mM Pyruvate (11360070, Gibco), and 0.87
583 mg/mL NaCl in DMEM (11885084, Gibco).
584 **LTR (Long-Term Retina) media**: 25% F12 (11765062, Gibco) with 2% B27
585 Supplement (50X) (17504044, Gibco), 10% heat inactivated FBS (16140071, Gibco),
586 1mM Sodium Pyruvate,1% NEAA, 1% Glutamax and 1 mM taurine (T-8691, Sigma) in
587 DMEM (11885084, Gibco).

588 **RPMI + supplement media:** 10% heat inactivated FBS (16140071, Gibco), 2.5%
589 penicillin (30-002-CI, Corning) in RPMI Medium 1640 (11875135, Gibco).
590 **HEK293 + supplement media**: 10% heat inactivated FBS (16140071, Gibco),
591 2.5% penicillin (30-002-CI, Corning) in DMEM 4.5g/L D-glucose, L-glutamine
592 (11965084, Gibco).
593 **Retinoic acid treatment:** For organoids, 1.04 μM all-trans retinoic acid (ATRA;
594 R2625; Sigma) in LTR.
595 **Thyroid hormone treatment:** For Weri-Rb1 cells, 100 nM T3 (T6397, Sigma) in
596 RPMI + supplement media.
597
598 **Organoid differentiation**
599 Organoids were differentiated from H7 WA07, H7iCas9 ESCs, or EP1.1 iPSCs
600 as described in Eldred *et al.* 2018 with minor variations (**Fig. S5**)[2].
601 Pluripotent stem cells were well-maintained. Cultures with minimal to no
602 spontaneous differentiation were used for aggregation. To aggregate, cells were
603 passaged in Accutase (SCR005, Sigma) at 37°C for 12 min to ensure complete
604 dissociation. Cells were seeded in 50 μLs of mTeSR1 at 3,000 cells/well into 96-well
605 ultra-low adhesion round bottom Lipidure coated plates (51011610, NOF) or ultra-low
606 attachment microplate (7007, Corning). Cells were placed in hypoxic conditions (10%
607 CO2 and 5% O2) for 24 hours to enhance survival. Cells naturally aggregated by gravity
608 over 24 hours.
609 On day 1, cells were moved to normoxic conditions (5% CO2). On days 1-3, 50
610 μLs of BE6.2 media containing 3 μM Wnt inhibitor (IWR1e: 681669, EMD Millipore) and

611 1% (v/v) Matrigel were added to each well. On days 4-9, 100 µLs of media were
612 removed from each well, and 100 µLs of media were added. On days 4-5, BE6.2 media
613 containing 3 µM Wnt inhibitor and 1% Matrigel was added. On days 6-7, BE6.2 media
614 containing 1% Matrigel (354230, BD Biosciences) was added. On days 8-9, BE6.2
615 media containing 1% Matrigel and 100 nM Smoothened agonist (SAG: 566660, EMD
616 Millipore) was added.

617 On day 10, aggregates were transferred to 15 mL tubes, rinsed 3X in 5mL
618 DMEM (11885084, Gibco), and resuspended in BE6.2 with 100 nM SAG in untreated 10
619 cm polystyrene petri dishes. From this point on, media was changed every other day.
620 Aggregates were monitored and manually separated if stuck together or to the bottom of
621 the plate.

622 On days 13-16, LTR media with 100 nM SAG was added. On day 16, retinal
623 vesicles were manually dissected using sharpened tungsten needles. After dissection,
624 cells were transferred into 15 mL tubes and washed 2X with 5 mLs of DMEM. On days
625 16-20, cells were maintained in LTR and washed 2X with 5 mLs of DMEM, before being
626 transferred to new plates to wash off dead cells. To increase survival and differentiation,
627 1.04 µM all-trans retinoic acid (ATRA; R2625; Sigma) was added to LTR medium from
628 days 20-43. Additional time windows of 1.04 µM were added depending on
629 experimental conditions. 10 µM gamma-secretase inhibitor (DAPT, 565770, EMD
630 Millipore) was added to LTR from days 28-42. Organoids were grown at low density (10-
631 20 per 10 cm dish) to reduce aggregation. Periodically, organoids were culled from the
632 plate based on absence of clear laminal structure indicating proper retinal organoid
633 growth.

634 **RNA-Seq experiments**

635 EP1 iPSC-derived organoids were previously grown and analyzed for Eldred *et*
636 *al.* 2018 at time points ranging from day 10 to day 250 of differentiation[2]. Samples were
637 taken at day 10 (N=3), day 20 (N=2), day 35 (N=3), day 69 (N=3), day 111 (N=3), day
638 128 (N=3), day 158 (N=2), day 173 (N=3), day 181 (N=3), day 200 (N=3), and day 250
639 (N=3).

640 H7 ESC-derived organoids were taken at day 329 (N=3).

641 Weri-Rb-1 samples were grown in control RPMI + supplement media or T3-
642 treated RPMI + supplement media for four days (N=1).

643 RNA from individual samples was extracted using the Zymo Direct-zol RNA
644 Microprep Kit (R2062, Zymo Research) according to manufacturer's instructions.
645 Libraries were prepared using the Illumina TruSeq stranded mRNA kit and sequenced
646 on an Illumina NextSeq 500 with single 75 bp reads.

647

648 **RNA sequencing analysis**

649 **Quantification of Opsin Expression in Human Fetal Retina Samples from[3,4]:**
650 Expression of opsin genes was directly quantified from FASTQ files using Kallisto
651 0.44.0. The kallisto index was generated from the Gencode V27 human transcriptome,
652 with the default kmer setting of 31. Reads were quantified in single-ended mode with a
653 specified length of 75 and standard deviation of 10.

654

655 **Analysis of Opsin Pileups:** To examine the reads mapped to each opsin
656 directly, reads were aligned to the opsin transcripts using Bowtie 2.3.4.3, and aligned

657 files were processed with samtools 1.7 to produce pileups around selected locations in
658 the transcripts. For the quantification of human samples, a Bowtie2 index was
659 generated from sequences ENST00000595290.5 and ENST00000369951.8 using the
660 default settings. Pileups were generated for transcript positions given in Table 1:
661

Exon	Base		Transcript position		Exon Position	Absolute Position	
	LW	MW	LW	MW		LW	MW
2	C	T	254	276	81	154150737	154187851
	A	G	360	382	187	154150843	154187957
	A	G	391	413	218	154150874	154187988
	C	A	407	429	234	154150890	154188004
4	T	C	749	771	110	154154684	154191798
	G	A	757	779	118	154154692	154191806
	C	G	758	780	119	154154693	154191807
	T	C	759	781	120	154154694	154191808
	A	G	766	788	127	154154701	154191815
5	A	G	880	902	75	154156369	154193483
	T	C	883	905	78	154156372	154193486
	T	G	885	907	80	154156374	154193488
	G	A	888	910	83	154156377	154193491
	A	T	890	912	85	154156379	154193493
	G	T	895	917	90	154156384	154193498
	C	A	901	931	104	154156398	154193512
	A	G	905	935	108	154156402	154193516
	T	C	940	970	143	154156437	154193551
	G	C	944	974	147	154156441	154193555
	A	T	978	1008	181	154156475	154193589

662
663

664 **Association Study**

665 **Subjects:** All experiments involving human subjects were conformed to the
666 principles expressed in the Declaration of Helsinki and were approved by the University
667 of Washington Human Subjects Review Committee. Subjects were 738 males who had
668 previously passed several standard tests for color vision deficiency, including Ishihara's
669 24-plate test, Richmond HRR 2002 edition, and the Neitz Test of Color Vision. Subjects
670 identified themselves as being either of African or African American ancestry (N=147),
671 Asian ancestry (N=108), Caucasian ancestry (N=362), Latino ancestry (N=23), Mixed
672 (N=62), Native American ancestry (N=13), South Asian ancestry (N=9), or Other/Not
673 Specified (N=14). The proportion of L cones, expressed as the percentage of L plus M
674 cones that were L, were determined for each subject from a combination of genetic
675 analysis and the flicker photometric electroretinogram (FP-ERG) as described in[5,6].
676 Briefly, the spectral sensitivity of the individual was measured using control and test
677 lights of specific wavelengths to illuminate a small portion of the retina. These conditions
678 were designed to eliminate rod and S-cone contributions. While the test lights were
679 flickered on and off, electrodes recorded the ERG neuronal responses to the stimulus.
680 The spectral sensitivity was determined by adjusting the intensity of the test light until
681 the ERG signal produced exactly matched that produced by the fixed intensity reference
682 light. A correction factor was applied to the estimated proportion of L cones to account
683 for the 1.5 times greater contribution to the FP-ERG signal for each M cone compared
684 to each L cone[7]. These data combined with genetic analysis of the L and M cone genes
685 to determine the spectral sensitivity of each opsin allowed for the determination of the
686 L:M cone ratio.

687 **DNA preparation, pull-down, and sequencing:** DNA was isolated from buccal
688 swabs or whole blood using PureGene DNA extraction kits as described in[8]. DNA was
689 then diluted to 10 ng/µL in low ETDA (USB corporation, #75793). DNA was sheared to
690 an average length of 250 bps using the Bioruptor® Pico (Diagenode). Samples were
691 stored on ice for 10-15 min prior to sonication. Sonication was performed for 7 cycles of
692 on for 15 seconds, off for 90 seconds. After 3 cycles, the samples were briefly
693 centrifuged before continuing with sonication for the remaining 4 cycles. Library
694 preparation and hybridization pull-downs were performed according to the SeqCap EZ
695 HyperCap Workflow User's Guide, version 2.0 following all recommended instructions.
696 Libraries were created using the KAPA Hyper Prep Kit (KAPA Biosystems, #KK8504),
697 using the KAPA Dual-Indexed Adapter Set (15 mM, KAPA Biosystems/Roche, #08 278
698 555 702). Probes for the pull-down were designed according to the Roche Nimble
699 Design software, targeting the gene regions listed in (**Fig. S2**). Samples were
700 sequenced on a Nova-seq, high-output, with 125 bp paired-end reads.
701
702 **Analysis:** Paired-end reads for 738 samples were aligned to the human
703 genome (build hg38) using BWA mem (v0.7.15) using default parameters. Duplicate
704 reads were marked using Picard (v2.9.2). Each region was subdivided into
705 nonoverlapping 1 kb windows starting at the upstream boundary using bedtools
706 (v2.29.2). Mapped reads were genotyped on a region-by-region basis using Freebayes-
707 parallel (v1.2.0), the argument '--use-best-n-alleles 4', and, for the region on
708 chromosome X, '-p 1'. Variant calls were filtered for quality greater than 10 times the
709 number of additional observations, at least one alternative allele read on each strand,

710 and at least two reads supporting the alternate allele balanced up- and downstream
711 using vcflib (v1.0.0). Duplicate variants were then removed. Variants were filtered with
712 PLINK (v1.90b6.12) for a minor allele frequency of at least 3.5% and a per-variant
713 genotyping rate of at least 90%. Variants were pruned using LDAK (v5.0) with a linkage
714 disequilibrium cutoff of $R^2 < 0.75$ within 100 kb windows. A kinship matrix was
715 calculated from the pruned variant set using LDAK, ignoring weights and a power of -1.
716 P-values were calculated in LDAK from the pruned variant set, using the first five
717 genotype eigenvectors as covariates to control for potential population stratification.
718 Significant variants were defined using an alpha of 0.05 after Bonferroni correction.
719

720 **Transfection of opsin cDNA into HEK293 cells**

721 HEK293 cells were passaged 24 hours prior to be <60% confluent on the day of
722 transfection. Transfection was done with the Lipofectamine® 3000 transfection kit
723 (L3000001, Invitrogen). For a 10 cm dish, 7.5 µL lipofectamine 3000 was mixed with
724 125 µL Opti-MEM (31985062, Thermo Fisher Scientific) at room temperature for 5
725 minutes. 5 µL of P3000, 0.5-1 µg DNA, and 125 µL Opti-MEM was mixed at room
726 temperature for 5 minutes. The two solutions were mixed and incubated at room
727 temperature for 10 minutes. Media was aspirated from HEK293 cells and replaced with
728 8 mL of prewarmed Opti-MEM. Lipofectamine mixture was mixed onto cells and
729 incubated at 37ºC in a HERAcell 150i or 160i 5% CO_2 incubator for 4-6 hours.
730 Transfection media was aspirated and replaced with HEK293 maintenance media
731 (DMEM/10% FBS/1X Penn/Strep) and allowed to recover overnight. Cells were allowed
732 to adhere to slides coated with 10% Poly-L-lysine solution (0.1% w/v in H_2O) (P8920,

733 Sigma) for 1-3h at 37ºC in a HERAcell 150i or 160i 5% CO_2 incubator (Thermo Fisher
734 Scientific). Cells were washed in 1x PBS and fixed in 10% neutral buffered formalin
735 (HT501128, Sigma) for 30 minutes. Slides were either used immediately for RNA *in situ*
736 or dried and stored at -80ºC.
737 Plasmids containing cDNA for *OPN1MW* and *OPN1LW* were purchased from
738 GenScript: NM_000513.2 (*OPN1MW*) and NM_020061.5 (*OPN1LW*).
739
740 **Human retina and organoid preparation and cryosectioning**
741 **Human retina:** Donor sample was flash frozen on dry ice 10.9 hours postmortem
742 and stored at -80C. The human eye was allowed to come to room temperature in 1X
743 PBS and the retina was dissected out of the eye. The retina was fixed for 45 minutes in
744 10% neutral buffered formalin (HT501128, Sigma) and washed in 1X PBS. Subsections
745 of retina were mounted in Tissue-Tek O.C.T. compound (4583, Sakura), placed on dry
746 ice to freeze, and stored at -80C. The retina was sectioned in 10 µm sections. Slides
747 were air dried for 6 hours to overnight with a post-fixation step of 15 minutes in 10%
748 neutral buffered formalin (HT501128, Sigma) and washed in 1X PBS. Slides were dried
749 and stored at -80C for less than 3 months before use.
750 **Organoid:** Organoids were fixed for 45 minutes in 10% neutral buffered formalin
751 (HT501128, Sigma) and washed in 1X PBS. Organoids were placed in a 25% sucrose
752 in 0.1 M phosphate buffer solution overnight, and then mounted in Tissue-Tek O.C.T.
753 compound (4583, Sakura), placed on dry ice to freeze, and stored at -80C. Organoids
754 were sectioned in 10 µm sections. Slides were air dried for 6 hours to overnight with a
755 post-fixation step of 15 minutes in 10% neutral buffered formalin (HT501128, Sigma)

756 and washed in 1X PBS. Slides were dried and stored at -80C for less than 3 months
757 before use.
758
759 **Organoid cell lines**
760 **No RA:** H7 ESC (N=3)
761 **Early RA:** H7 ESC (N=1), H7 iCas9 ESC (N=2)
762 **Late RA:** H7iCas9 ESC (N=5)
763
764 **RNA *in situ* hybridization**
765 BaseScope RNA *in situ* hybridization was performed according to manufacturer's
766 instructions and modified with several changes. Probe sequences were designed by
767 ACD Biotechne based on *OPN1MW* and *OPN1LW* mRNA sequences *NM_000513.2*
768 *NM_020061.5* from the human genome hg38.
769 Sections were allowed to come to room temperature from storage at -80C and
770 rehydrated in 1X PBS. Samples were pretreated according to manufacturer's
771 instructions: 10 minutes of RNAscope Hydrogen Peroxide followed by a wash in dH_2O
772 and then 2 washes in 1X PBS.
773 RNAscope Protease III was applied at a 1:15 dilution in 1X PBS for 15 minutes in
774 a humid chamber for HEK293 cells. RNAscope Protease IV was applied for 20 minutes
775 in a humid chamber for organoids and human eye samples. Samples were washed in
776 1X PBS twice.
777 Probes were added at the manufacturer suggested concentration to samples in

778 the HybEZ Humidity Control rack with lid and insert into the HybEZ oven for 2 hours at
779 40C. Samples were washed twice in 1x RNAscope wash buffer for 2 min.
780 Amplification and development washes were done with the manufacturer
781 reagents without change to the recommended concentrations. All washes were done in
782 the HybEZ Humidity Control rack with lid and insert, either at room temperature (RT) or
783 at 40C in the HybEZ oven. Each wash was done at the following temperatures and time
784 lengths:
785

Reagent	Temperature (°C)	Time (min)
AMP 1	40	30
AMP 2	40	30
AMP 3	40	15
AMP 4	40	30
AMP 5	40	30
AMP 6	40	15
AMP 7	RT	30
AMP 8	RT	15
RED-A/B	RT	10
AMP 9	40	15
AMP 10	40	15
AMP 11	RT	30
AMP 12	RT	15
GREEN-A/B	RT	10

786
787 2X 2 min washes in 1X RNAScope Buffer were conducted between each reagent wash.
788 The final wash was in tap water. Slides were baked for a minimum of 30 minutes at 65C
789 in the HybEZ oven. Samples were preserved with VectaMount (Vector Laboratories, H-
790 5000) mounting media and a sealed coverslip.
791
792
793

794 **Imaging**

795 **HEK293:** Cells were imaged using an EVOS XL Core Cell imaging system

796 (ThermoFisher).

797 **Organoids and human retina:** Samples were imaged using a Zeiss LSM 980

798 color camera system.

799

800 **Quantification**

801 **HEK293:** All individual cells were counted manually.

802 **Organoids:** All serially sectioned organoids were imaged and counted manually.

803 Organoids that had fewer than 150 cones (n ≤150) were removed from our analysis.

804 Statistical tests are listed in figure legends. All error bars represent SEM.

805

806

807 **Methods References**

808 1 Wahlin, K. J. *et al.* Photoreceptor Outer Segment-like Structures in Long-Term 3D
809 Retinas from Human Pluripotent Stem Cells. *Sci Rep* **7**, 766, doi:10.1038/s41598-
810 017-00774-9 (2017).

811 2 Eldred, K. C. *et al.* Thyroid hormone signaling specifies cone subtypes in human
812 retinal organoids. *Science* **362**, doi:10.1126/science.aau6348 (2018).

813 3 Pinelli, M. *et al.* An atlas of gene expression and gene co-regulation in the human
814 retina. *Nucleic Acids Res* **44**, 5773-5784, doi:10.1093/nar/gkw486 (2016).

815 4 Hoshino, A. *et al.* Molecular Anatomy of the Developing Human Retina. *Dev Cell*
816 **43**, 763-779 e764, doi:10.1016/j.devcel.2017.10.029 (2017).

817 5 Carroll, J., Neitz, J. & Neitz, M. Estimates of L:M cone ratio from ERG flicker
818 photometry and genetics. *J Vis* **2**, 531-542, doi:10.1167/2.8.1 (2002).

819 6 McMahon, C., Carroll, J., Awua, S., Neitz, J. & Neitz, M. The L:M cone ratio in
820 males of African descent with normal color vision. *J Vis* **8**, 5 1-9, doi:10.1167/8.2.5
821 (2008).

822 7 Hofer, H., Carroll, J., Neitz, J., Neitz, M. & Williams, D. R. Organization of the
823 human trichromatic cone mosaic. *J Neurosci* **25**, 9669-9679,
824 doi:10.1523/JNEUROSCI.2414-05.2005 (2005).

825 8 Gunther, K. L., Neitz, J. & Neitz, M. Nucleotide polymorphisms upstream of the X-
826 chromosome opsin gene array tune L:M cone ratio. *Vis Neurosci* **25**, 265-271,
827 doi:10.1017/S0952523808080280 (2008).

828

Figure 1

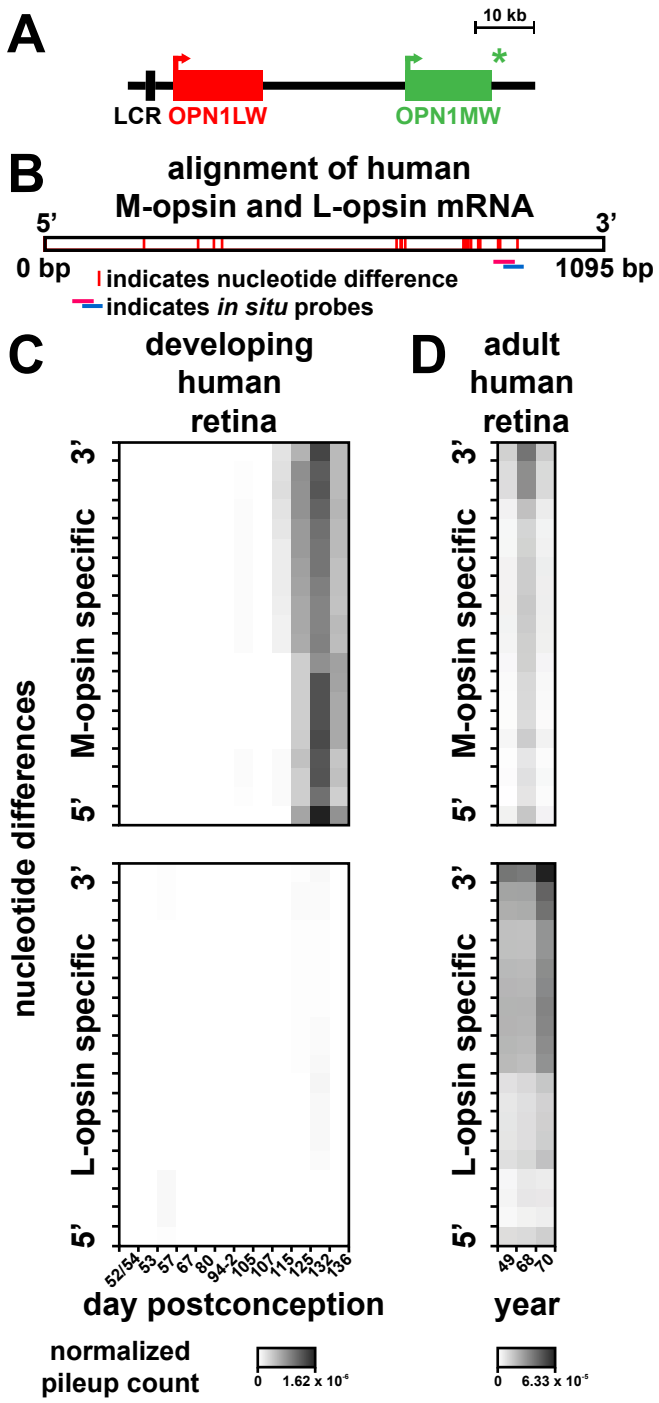
A
10 kb
LCR OPN1LW
OPN1MW
B
alignment of human
M-opsin and L-opsin mRNA
5'
3'
0 bp
1095 bp
indicates nucleotide difference
indicates in situ probes
C
developing
human
retina
D
adult
human
retina
nucleotide differences
M-opsin specific
L-opsin specific
5'
3'
52/54
53
57
67
80
94-2
105
107
115
125
132
136
day postconception
49
68
70
year
normalized
pileup count
0
1.62 x 10-5
6.33 x 10-5

829 **Fig. 1. *M-opsin* is expressed before *L-opsin* in fetal human retinas.**

830 **(A)** Human *L/M-opsin* locus. LCR = locus control region; *OPN1LW* (red) = *L-opsin*,

831 *OPN1MW* (green) = *M-opsin*. * indicates that the copy number of *OPN1MW* genes is

832 variable in the human population.

833 **(B)** Alignment of human *M-opsin* and *L-opsin* mRNA. Red bar = nucleotide difference.

834 Horizontal pink and blue lines = location of the *in situ* probes (as in **Fig. 3A)**.

835 **(C-D)** *M-* and *L-opsin* expression. Heatmap indicates total pileup count normalized to

836 total read count. Each square indicates one nucleotide difference in *M-* or *L-opsin.*

837 **(C)** Human embryonic and fetal retinas analyzed from [41] (n = 1 for each timepoint;

838 except 94-2 where n = 2). 52/54 = exact date is unclear.

839 **(D)** Human adult retinas (n = 1 for each timepoint) analyzed from [42].

Figure 2

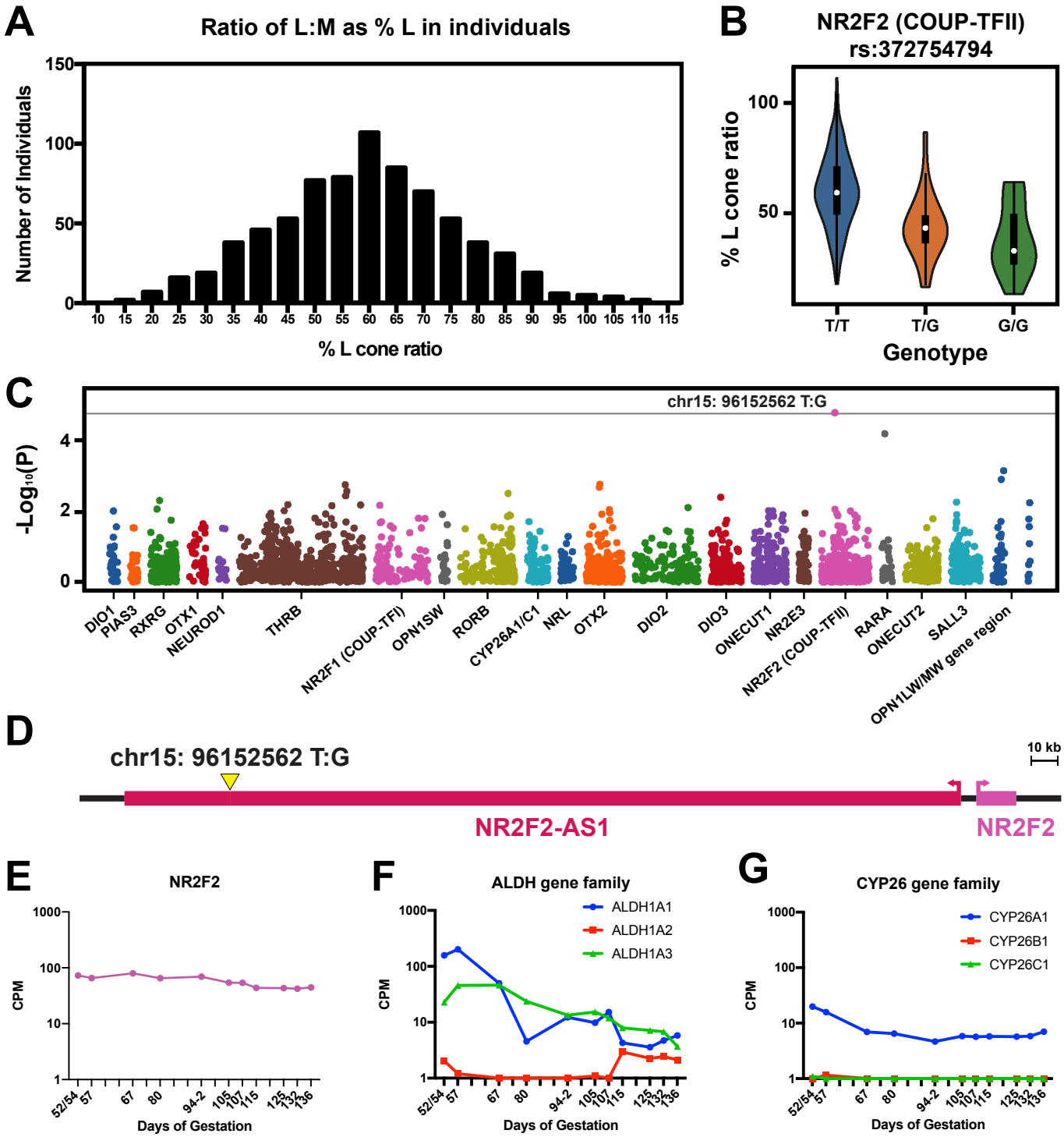
A
Ratio of L:M as % L in individuals
Number of Individuals
% L cone ratio
B
NR2F2 (COUP-TFII)
rs:372754794
% L cone ratio
T/T
T/G
G/G
Genotype
C
chr15: 96152562 T:G
-Log10(P)
DIO1
PIAS3
RXRG
OTX1
NEUROD1
THRB
NR2F1 (COUP-TFI)
OPN1SW
RORB
CYP26A1/C1
NRL
OTX2
DIO2
DIO3
ONECUT1
NR2E3
NR2F2 (COUP-TFII)
RARA
ONECUT2
SALL3
OPN1LW/MW gene region
D
chr15: 96152562 T:G
10 kb
NR2F2-AS1
NR2F2
E
NR2F2
CPM
Days of Gestation
F
ALDH gene family
ALDH1A1
ALDH1A2
ALDH1A3
CPM
Days of Gestation
G
CYP26 gene family
CYP26A1
CYP26B1
CYP26C1
CPM
Days of Gestation

840 **Fig. 2. SNPs in RA signaling regulators are associated with changes in L:M cone**
841 **ratios.**
842 **(A)** Histogram of the ratios of % L from 738 human males with normal color vision.
843 **(B)** Violin plots of % L cone ratios for the genotypes of the significant polymorphism in
844 *NR2F2*.
845 **(C)** Manhattan plot of the genetic variant p-values. Genetic variants above the gray line
846 (Bonferroni corrected threshold) are considered significant ($p < 0.05$).
847 **(D)** *NR2F2* gene locus. *NR2F2* gene (pink); *NR2F2* antisense RNA (dark pink). Yellow
848 arrow denotes the location of the SNP.
849 **(E-G)** Human fetal retina expression for **(E)** *NR2F2*, **(F)** *ALDH1A1, A2,* and *A3,* and **(G)**
850 *CYP26A1, B1, and C1* from [41]. CPM = log counts per million.

Figure 3

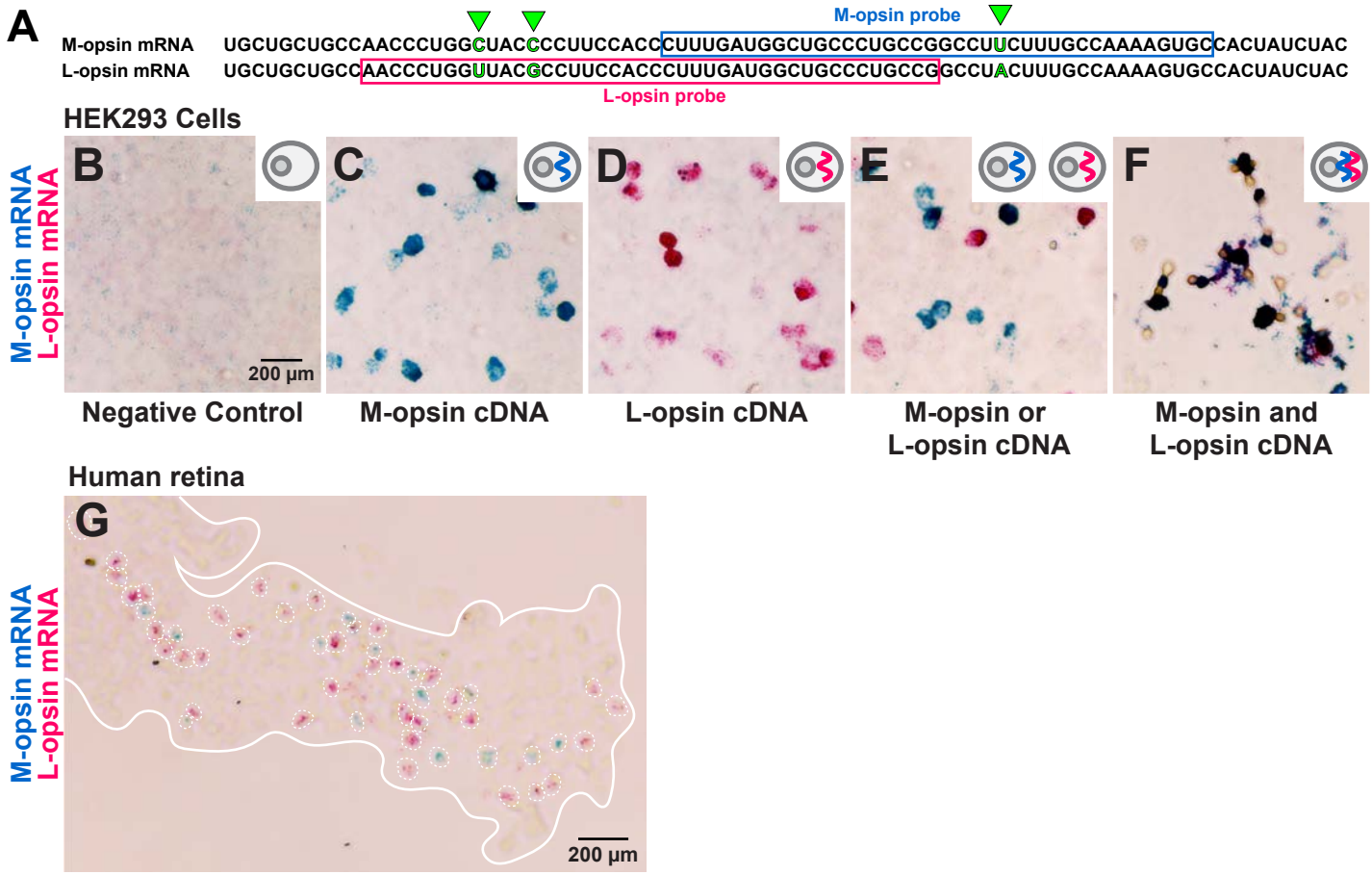
A
M-opsin probe
M-opsin mRNA UGCUGCUGCCAACCCUGGCUACCCCUUCCACCCUUUGAUGGCUGCCCUGCCGGCCUUCUUUGCCAAAAGUGCCACUAUCUAC
L-opsin mRNA UGCUGCUGCCAACCCUGGUUACGCCUUCCACCCUUUGAUGGCUGCCCUGCCGGCCUACUUUGCCAAAAGUGCCACUAUCUAC
L-opsin probe
HEK293 Cells
M-opsin mRNA
L-opsin mRNA
B
C
D
E
F
200 µm
Negative Control
M-opsin cDNA
L-opsin cDNA
M-opsin or L-opsin cDNA
M-opsin and L-opsin cDNA
Human retina
G
M-opsin mRNA
L-opsin mRNA
200 µm

851 **Fig 3. Visualization of *M-* and *L-opsin* mRNA.**

852 **(A)** Alignment of portions of exon 5 from *M-* and *L-opsins*. *in situ* hybridization probe

853 binding sites are indicated by blue (*M-opsin*) and pink (*L-opsin*) boxes. Green

854 arrowheads indicate 3 nucleotide differences.

855 **(B-F)** HEK293 cells probed for both *M-opsin* and *L-opsin*. Insets indicate a schematic of

856 the transfected plasmid; blue = *M-opsin* cDNA; pink = *L-opsin* cDNA.

857 **(B)** No cDNA was transfected.

858 **(C)** *M-opsin* cDNA was transfected.

859 **(D)** *L-opsin* cDNA was transfected.

860 **(E)** Either *M-* or *L-opsin* cDNA was transfected independently and then the cells were

861 mixed.

862 **(F)** *M-* and *L-opsin* cDNAs were co-transfected.

863 **(G)** 10 μm section of adult human retina probed for both *M-opsin* and *L-opsin*; blue = *M-*

864 *opsin*; pink = *L-opsin*.

Figure 4

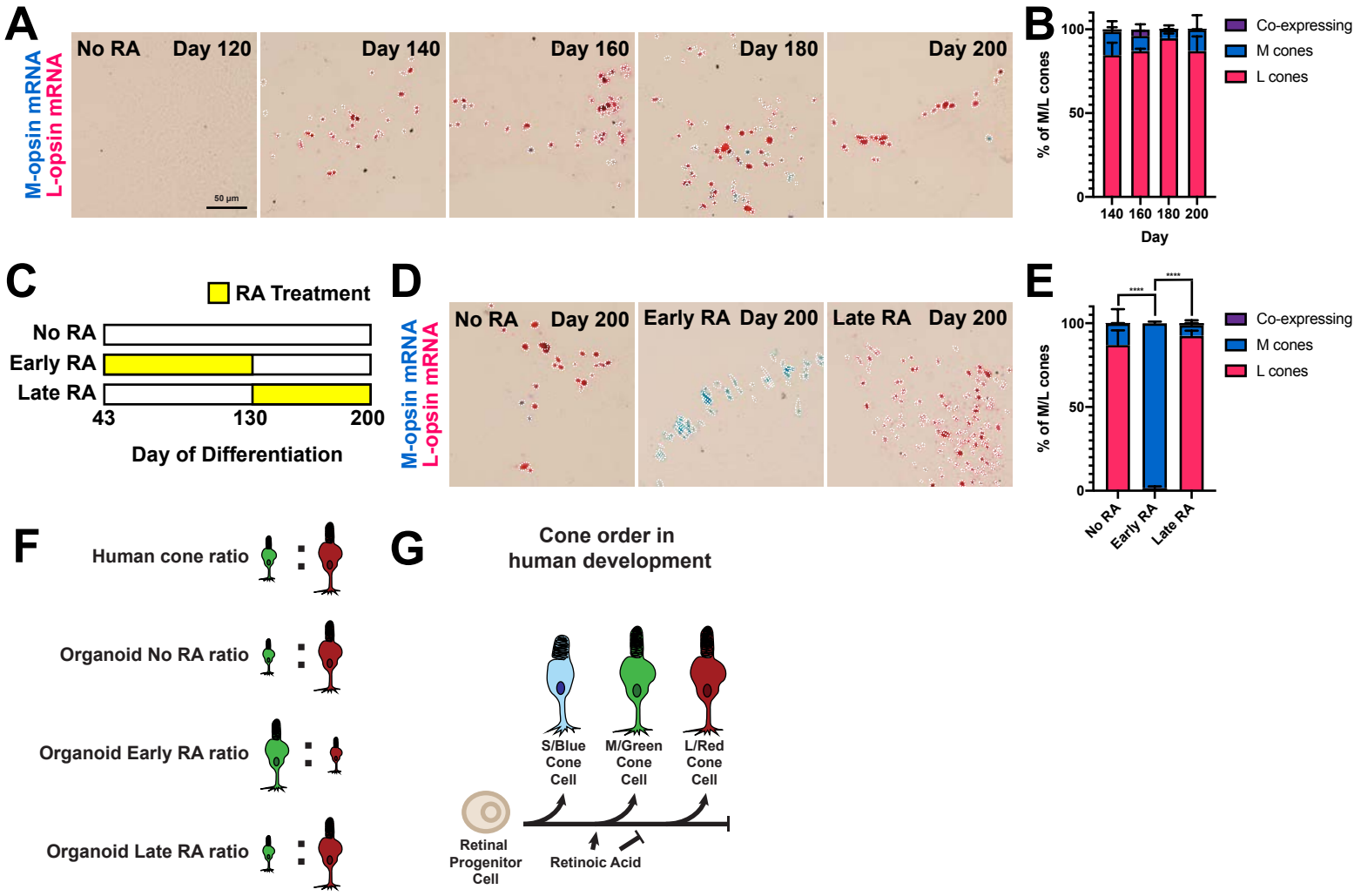
A
M-opsin mRNA
L-opsin mRNA
No RA
Day 120
Day 140
Day 160
Day 180
Day 200
50 µm
B
% of M/L cones
100
50
0
140 160 180 200
Day
Co-expressing
M cones
L cones
C
RA Treatment
No RA
Early RA
Late RA
43
130
200
Day of Differentiation
D
M-opsin mRNA
L-opsin mRNA
No RA Day 200
Early RA Day 200
Late RA Day 200
E
% of M/L cones
100
50
0
****
****
No RA
Early RA
Late RA
Co-expressing
M cones
L cones
F
Human cone ratio
Organoid No RA ratio
Organoid Early RA ratio
Organoid Late RA ratio
G
Cone order in
human development
S/Blue
Cone
Cell
M/Green
Cone
Cell
L/Red
Cone
Cell
Retinal
Progenitor
Cell
Retinoic Acid

865 **Fig. 4. RA signaling induces *M-opsin* and inhibits *L-opsin* early in human retinal**
866 **organoids.**
867 **(A)** *M-opsin* (blue) and *L-opsin* (pink) expression in 'No RA' human retinal organoids.
868 White outlines indicate *M-* or *L-opsin*-expressing cells.
869 **(B)** Quantification of A. For day 120, organoids had fewer than 150 M or L cones (N=3)
870 (**Fig. S6A**). For day 140, 160, 180, and 200, organoids had greater than 150 M or L
871 cones (**Fig. S6A**). For day 140, N=4; for day 160, N=3; for day 180, N=3; and for day
872 200, N=3. Tukey's multiple comparisons test: no significance. Error bars indicate SEM.
873 Data for 'No RA Day 200' are from the same experiment as in **Fig. 4E**.
874 **(C)** Yellow bars indicate temporal windows of RA addition. 'No RA' = no RA addition
875 after day 43. 'Early RA' = RA addition on days 43-130. 'Late RA' = RA addition on days
876 130-200.
877 **(D)** *M-opsin* (blue) and *L-opsin* (pink) expression in organoids grown in 'No RA', 'Early
878 RA', and 'Late RA' conditions. White outlines indicate *M-* or *L-opsin*-expressing cells.
879 **(E)** Quantification of D. For 'No RA', N = 3; for 'Early RA', N=3; and for 'Late RA', N=5.
880 Tukey's multiple comparisons test: 'No RA' L-opsin versus 'Early RA' L-opsin P <
881 0.0001; 'Early RA' L-opsin versus 'Late RA' L-opsin P < 0.0001. Error bars indicate
882 SEM. Data for 'No RA Day 200' are from the same experiment as in **Fig. 4B**.
883 **(F)** Summary of M:L cone ratios in human retinas and retinal organoids.
884 **(G)** Model for temporal specification of human cone cell subtypes.

Supplemental 1

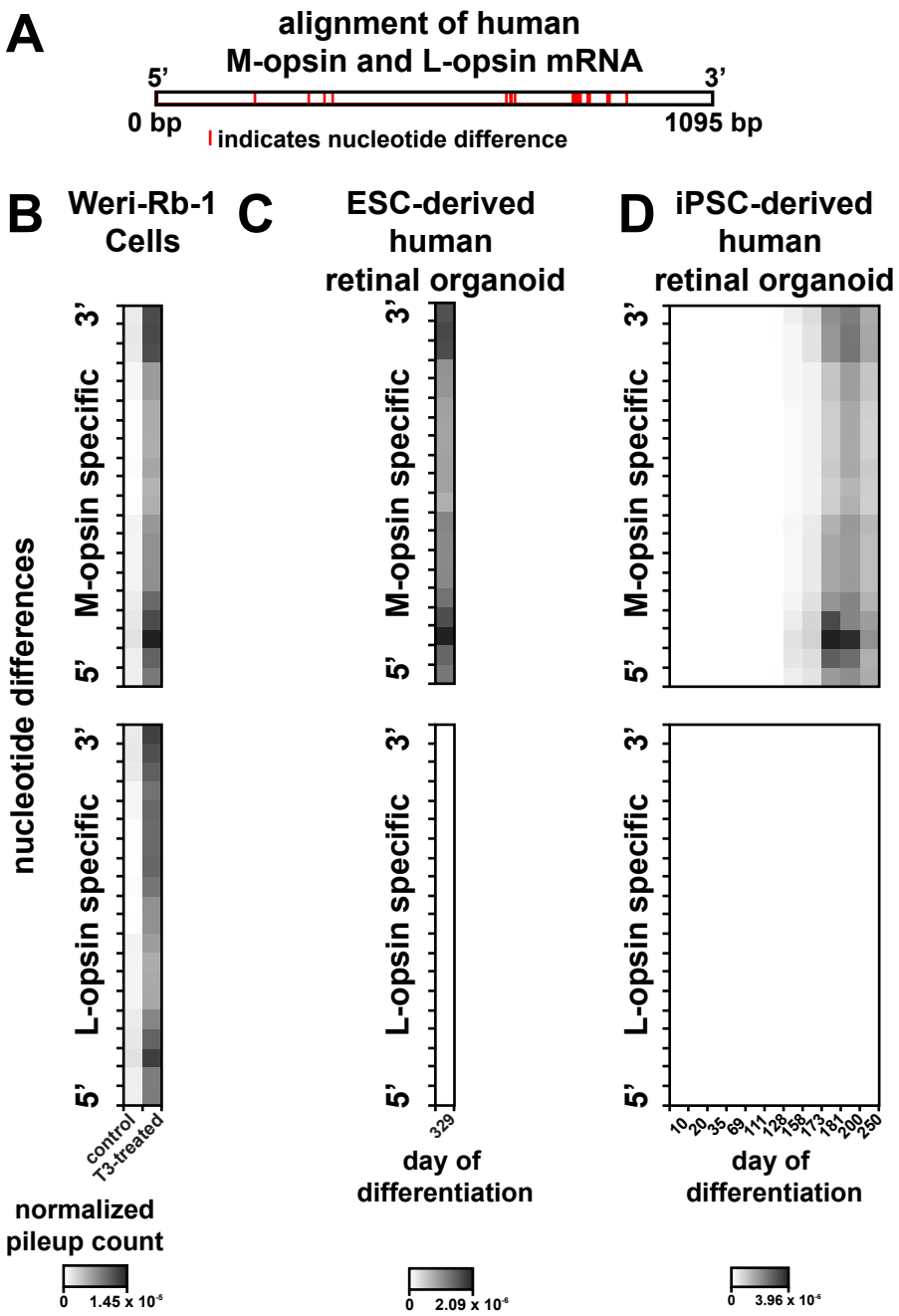

885 **Supplemental Fig. 1. *M-opsin* and *L-opsin* mRNA expression in retinoblastoma**
886 **cells and human retinal organoids.**
887 **(A)** Alignment of human *M-opsin* and *L-opsin* mRNA. Red bar = nucleotide difference.
888 (**B to D)** *M-* and *L-opsin* expression. Heatmap indicates total pileup count normalized to
889 total read count. Each square indicates one nucleotide difference in *M-* or *L-opsin.*
890 **(B)** Control- and T3-treated Weri-Rb-1 retinoblastoma cells (N=1 for each timepoint).
891 **(C)** Human ESC-derived retinal organoids. RA treatment = 'Early' days 43-130. (N=3).
892 **(D)** Human iPSC-derived retinal organoids. RA treatment = 'Early' days 43-130. (N=3
893 for each timepoint; except day 20 and 158 where N=2) analyzed from [36].

Supplemental 2

List of genes in association study and gene coordinates

Gene of Interest	chr#	Start	End
DIO1	chr1	53879779	53926574
PIAS3	chr1	145832505	145876560
RXRG	chr1	165346715	165499575
OTX1	chr2	63035597	63131383
NEUROD1	chr2	181647107	181693113
THRB	chr3	23970618	24697919
NR2F1 (COUP-TFI)	chr5	93319359	93628069
OPN1SW	chr7	128759936	128801444
RORB	chr9	74405551	74732495
CYP26A1/C1	chr10	93049490	93167890
NRL	chr14	24068098	24141275
OTX2	chr14	56755757	56970833
DIO2	chr14	80137530	80506478
DIO3	chr14	101447117	101623452
ONECUT1	chr15	52686989	52880012
NR2E3	chr15	71773279	71832289
NR2F2 (COUP-TFII)	chr15	96074584	96352953
RARA	chr17	40294657	40370655
ONECUT 2	chr18	57358933	57558283
SALL3	chr18	78908993	79079394
LW/MW gene region	chrX	154087755	154305671

894 **Supplemental Fig. 2. Genes tested in association study.**

895 Gene names and corresponding chromosome coordinates for assembly hg38.

Supplemental 3

A

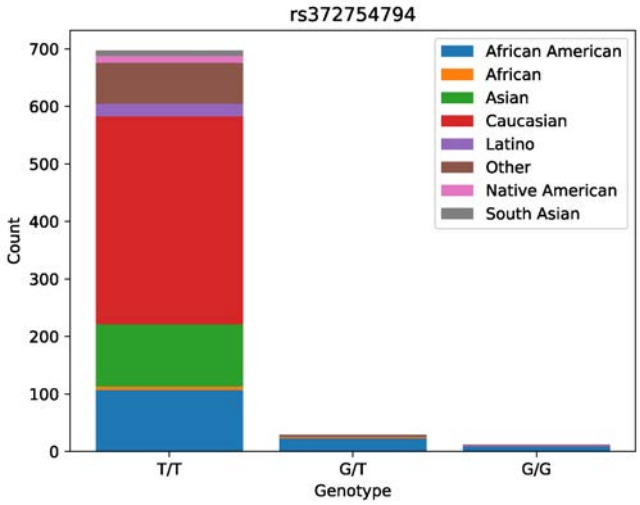

C

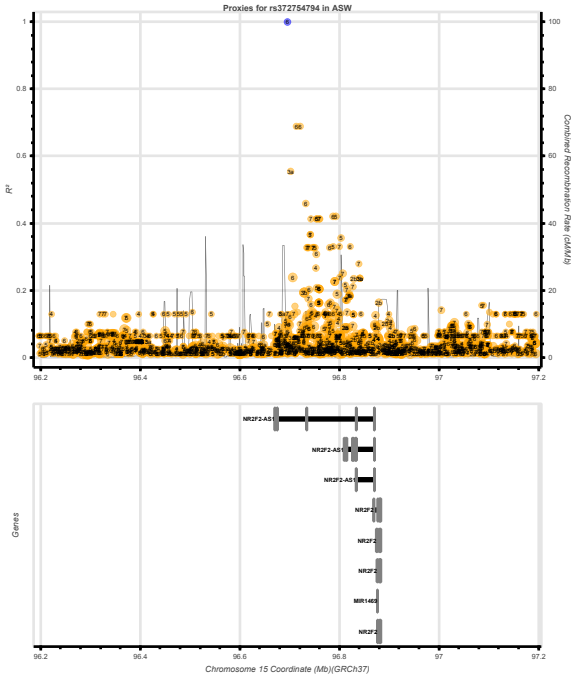

B

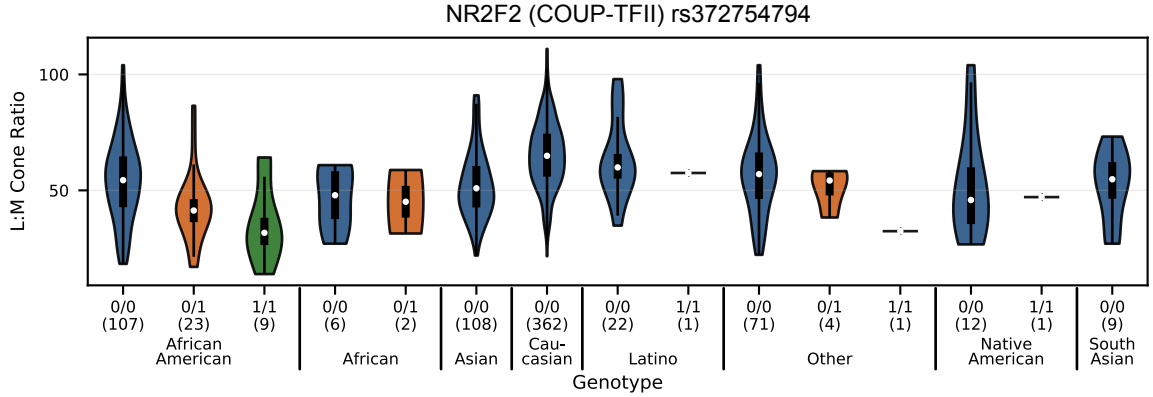

D

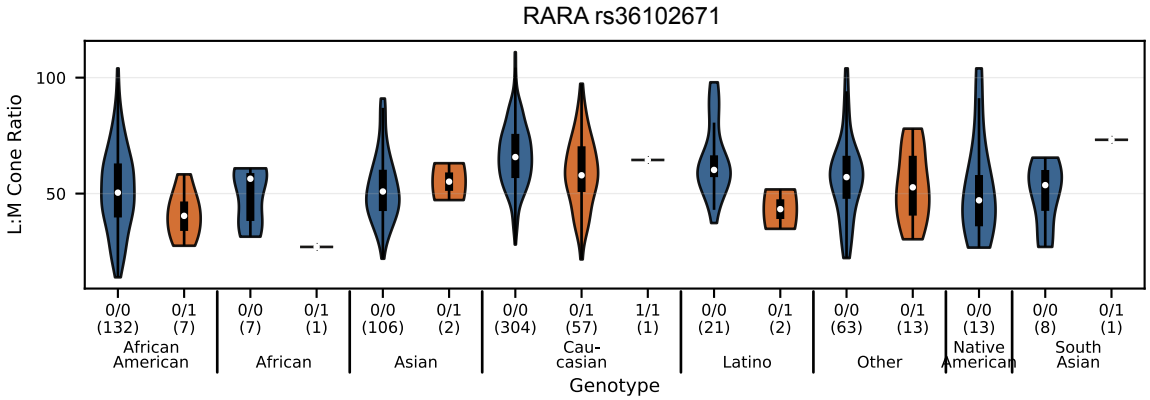

E

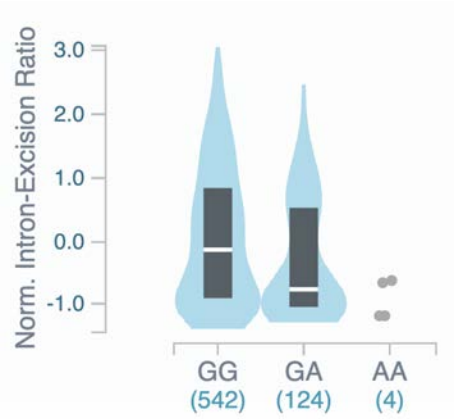

F

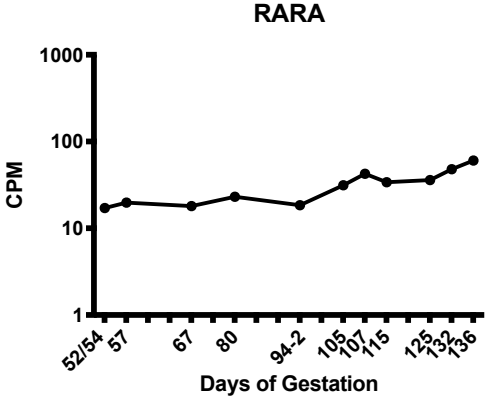

896 **Supplemental Fig. 3. Association study**

897 **(A)** Minor (G) allele ratio by ancestry.

898 **(B)** Association of L:M ratio and rs372754794 restricted to ancestry.

899 **(C)** Local LD plot for rs37275494 restricted to African American (ASW) populations.

900 **(D)** Association of L:M ratio and rs36102671 restricted to ancestry.

901 **(E)** rs36102671 association with altered splicing of RARA in whole blood from the

902 Genotype Tissue Expression Project (GTEx).

903 **(F)** Human fetal retina expression for *RARA* from [41]. CPM = log counts per million.

Supplemental 4

Transfection Condition	M- and L-opsin staining		
	M +	L +	Both +
Neg. Control	0	2	0
M-opsin	16,477	3	0
L-opsin	3	7,047	0
M- or L-opsin	230	463	0
M- and L-opsin	1,159	608	2,007

904 **Supplemental Fig. 4. Quantification of HEK293 cells expressing *M-opsin* and/or *L-***

905 ***opsin* expression.** Quantification of **Fig. 3B-F** (N=3 for each condition).

Supplemental 5

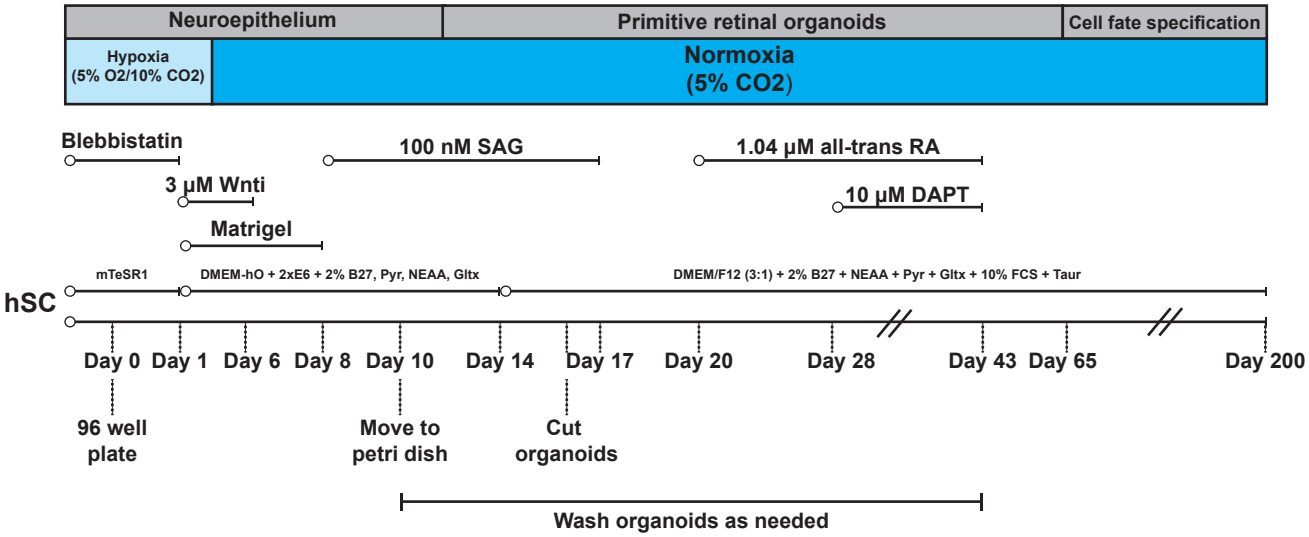

906 **Supplemental Fig. 5. Human retinal organoid protocol.** Standard conditions for human

907 retinal organoid differentiation, adapted from [36].

Supplemental 6

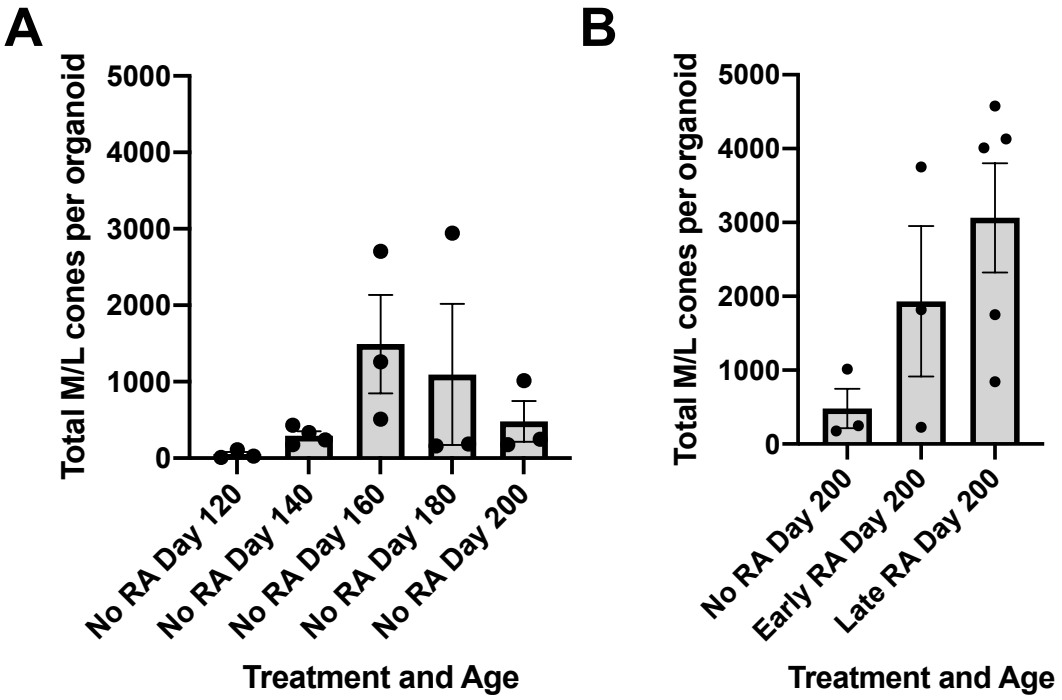

908 **Supplemental Fig. 6. Total M/L cone densities per organoid.**

909 **(A-B)** Quantification of total M/L cones per organoid. RA treatment conditions and
910 organoid age (as in **Fig. 4**) are listed on the X axis. Error bars indicate SEM. Individual
911 circles represent individual trials. 'No RA Day 200' repeated on both graphs. No significant
912 difference using Tukey's multiple comparisons test.